UNIVERSITÀ DEGLI STUDI DI PADOVA
Dipartimento di Biologia

SCUOLA DI DOTTORATO DI RICERCA IN: Bioscienze e Biotecnologie

INDIRIZZO: Biotecnologie

CICLO XXV

Mechanisms of atlastin-mediated membrane fusion and identification of atlastin functional partners involved in Endoplasmic Reticulum dynamics using *Drosophila* as a model.

Direttore della Scuola: Ch.mo Prof. Giuseppe Zanotti

Coordinatore d'indirizzo: Ch.mo Prof. Giorgio Valle

Supervisore: Ch.mo Prof. Elisabetta Bergantino

Co-supervisore: Dott. Andrea Daga

Dottorando: Camilla Andreazza

INDEX

ABSTRACT

Biogenesis and maintenance of the Endoplasmic Reticulum (ER) require membrane fusion. ER homotypic fusion is driven by the large GTPase atlastin, however, the mechanisms governing atlastin-mediated membrane fusion are unknown.

Using a structure-function analysis we investigated the mechanistic basis of nucleotide-dependent membrane fusion by *Drosophila* atlastin. Domain analysis of atlastin shows that a conserved region of the C-terminal cytoplasmic tail is absolutely required for fusion activity. Atlastin lacking the C-terminal domain is incapable of driving membrane fusion. When functional *Drosophila* atlastin is expressed, the normally reticular ER is lost and variably sized puncta are now stained with ER markers. However, overexpressing an ER localized truncated version of atlastin essentially does not disrupt ER morphology demonstrating that truncation results in a less- or non-functional protein. Deletion analysis has allowed to establish that a middle domain folded as a 3-helix bundle (3HB) is important for oligomerization. Mutations disrupting the structure of the helices within the 3HB inactivate atlastin by preventing tethering and the subsequent fusion of ER membranes. Furthermore, increasing the distance of atlastin complex formation from the membrane inhibits fusion, suggesting that this distance is crucial for atlastin to promote fusion.

Recently it has been shown that atlastin interacts with other ER tubule-forming proteins such as reticulon and REEP/Yop/DP1 families. We found that in *Drosophila* DP1 and reticulon interact genetically with atlastin. The lethality associated with null atlastin mutations is largely suppressed by the simultaneous loss of reticulon function. Furthermore, the hyperfusion phenotype caused by atlastin overexpression in COS-7 cells is rescued by co-expression of DP1 or reticulon. This result is supported by experiment in the fly eye. Expression of atlastin in the eye causes a small and rough eye phenotype. Overexpression of DP1 in an eye simultaneously expressing atlastin resulted in the rescue of the atlastin-dependent phenotype. Instead, loss of reticulon exacerbates the rough eye phenotype caused by atlastin overexpression. These data show that atlastin exibits a strong, antagonistic interaction with both reticulon and DP1 suggesting that these proteins are likely to exert opposing functions to regulate ER structure. We speculate that a balance between atlastin, reticulon, and DP1 activities is important in maintaining and determining the morphology of the ER.

RIASSUNTO

La biogenesi e il mantenimento del Reticolo Endoplasmatico (ER) richiedono fusione delle membrane. La fusione omotipica delle membrane del ER dipende dalla GTPasi atlastina, tuttavia i meccanismi che governano il processo di fusione mediato da questa proteina sono ancora sconosciuti.

Attraverso un'analisi struttura-funzione, abbiamo esaminato i meccanismi alla base del processo di fusione nucleotide-dipendente di atlastina nell'organismo modello *Drosophila melanogaster*. L'analisi dei domini di atlastina mostra che una regione conservata nella coda citoplasmatica C-terminale è indispensabile per la sua attività fusogena. Atlastina priva del dominio C-terminale non permette la fusione delle membrane. L'espressione di atlastina wild-type di *Drosophila* causa alterazione del caratteristico fenotipo reticolare del ER e marcatori del reticolo evidenziano dilatazioni delle membrane reticolari di varie dimensioni. Al contrario, l'espressione di atlastina tronca della regione C-terminale non altera la morfologia del ER dimostrando che questa forma troncata è poco o non funzionale *in vivo*.

L'espressione di atlastina tronca ha permesso di identificare un dominio intermedio costituito da un fascio di tre eliche che sono importanti per l'oligomerizzazione di atlastina. Mutazioni che distruggono la struttura delle alfa-eliche di questo dominio inattivano atlastina prevenendo l'avvicinamento e la conseguente fusione delle membrane del reticolo endoplasmatico. Inoltre, l'aumento della distanza di formazione del complesso di atlastina dalle membrane destinate a fondersi inibisce la fusione, suggerendo che questa distanza è cruciale per atlastina per promuovere la fusione.

Recentemente è stato visto che atlastina interagisce con altre proteine coinvolte nel determinare la morfologia del ER appartenenti alle famiglie reticulon e REEP/Yop/DP1. I nostri studi hanno dimostrato che DP1 e reticulon interagiscono funzionalmente con atlastina. La letalità dovuta a mutazione nulla di atlastina è recuperata dalla simultanea perdita di funzione di reticulon. Inoltre, il fenotipo di iperfusione causato da sovraespressione di atlastina in cellule COS-7 è recuperato co-esprimendo DP1 o reticulon. Questo risultato è supportato da esperimenti nell'occhio di *Drosophila*. Espressione di atlastina wild-type nell'occhio di *Drosophila* causa un occhio piccolo e rovinato. La sovraespressione simultanea di DP1 e atlastina nell'occhio risulta nel recupero del fenotipo causato dall'espressione di atlastina. Al contrario,

l'assenza di reticulon aumenta il fenotipo di occhio piccolo e rovinato dovuto a espressione di atlastina.

Questi risultati mostrano una forte interazione genetica antagonistica tra atlastina e reticulon o DP1, suggerendo che queste proteine esercitano funzioni opposte per regolare la struttura del ER. Ipotizziamo che un bilanciamento tra le attività di atlastina, reticulon e DP1 sia importante nel mantenimento e nel determinare la morfologia del reticolo endoplasmatico.

1 INTRODUCTION

1.1 Mechanism of membrane fusion and fission

Cellular membranes undergo continuous remodeling. Exocytosis and endocytosis, mitochondrial fusion and fission, entry of enveloped viruses into host cells and release of the newly assembled virions, cell-to-cell fusion and cell division, and budding and fusion of transport carriers all proceed via topologically similar, but oppositely ordered, membrane rearrangements (Kozlov *et al.*, 2010).

Membrane fusion occurs when two initially separate and apposed membranes merge into one by undergoing a sequence of intermediate transformations that seem to be conserved between disparate biological fusion reactions. This membrane rearrangement begins with local merger of only the contacting monolayers of the two membranes, while the distal monolayers remain separate. The initial lipid bridge between the membranes is referred to as the fusion stalk and signifies the first stage of fusion, called hemifusion. Stalk evolution ultimately leads to merger of the distal monolayers, resulting in the formation of a fusion pore that connects the volumes initially separated by the membranes and completes the membrane unification. The fusion pore must expand to a greater or smaller extent, depending on the specific biological context, for example, passage of small neurotransmitter molecules in the case of synaptic-vesicle exocytosis or a larger nucleocapsid in virus–cell fusion or the much larger nuclei in cell-to-cell fusion events.

Membrane fission – division of an initially continuous membrane into two separate ones – proceeds via the formation of a membrane neck, which is reminiscent of a fusion pore except that it narrows rather than expands. Theoretical analysis and a recent experimental study substantiate a scenario in which fission begins with self-merger of the inner monolayer of the neck membrane, which generates a fission stalk analogous to the fusion stalk. Subsequent self-merger of the outer monolayer of the membrane neck completes the fission process.

The fundamentally common feature of fusion and fission in these pathways is the formation of a membrane stalk at an intermediate stage of the reaction, which is followed by stalk decay. Obviously, stalk formation requires transient disruption of the membrane structure and hence is opposed by the powerful hydrophobic forces working to maintain continuity and integrity of any lipid assembly.

Membrane remodeling, either by fusion or fission, can occur if two physical requirements are fulfilled. First, the process must be energetically favorable overall. The system free energy before remodeling has to be higher than that after, which means that remodeling must result in relaxation of the free energy. Second, the energies of the intermediate structures formed transiently in the course of remodeling and representing kinetic barriers must be low enough to be overcome by system thermal fluctuations within a biologically relevant time. Membrane remodeling is driven and controlled by proteins that provide the required energy. Thus, it must be considered how proteins can generate the conditions for bilayer remodeling by changing the structure and physical state of lipid bilayers (Kozlov *et al.*, 2010).

1.1.1 Proteins driving fusion

Proteins can generate membrane curvature via different mechanisms. These include induction of lipid asymmetry of the membrane bilayer by flippases and lipid-modifying enzymes, molding of the membrane surface by rigid protein scaffolds, and insertion of hydrophobic protein domains into the lipid bilayer matrix. The latter is likely to be the most common mechanism. The essence of this mechanism lies in expansion of the polar head region of one of the membrane monolayers by shallow insertions in its matrix of small hydrophobic or amphipathic protein domains (Kozlov *et al.*, 2010).

Several energy barriers have to be overcome for fusion to occur. One energetically demanding process is to bring about the close apposition of two membranes, which requires protein clearance and the bringing together of repulsive membrane charges. The energy barriers related to curvature deformations during hemifusion-stalk and fusion-pore formation and expansion must also be overcome. The role of fusion proteins is to lower these barriers at the appropriate time and place to allow the regulation of the fusion process. Membrane fusion events generally require also molecules that locally disturb the lipid bilayers in order to reduce the energy barriers for fusion, and molecules that give directionality to the process. The driving force for membrane fusion can come from many sources, for example from the energy that is derived from protein-lipid interactions or from protein-protein interactions, and ultimately these reactions will have been primed by ATP. Directionality might be achieved by fusion protein folding. In addition, curvature stress that promotes fusion-stalk formation will be relieved during fusion-pore opening and expansion, again giving directionality to the process from the beginning (Martens and McMahon, 2008).

Membrane fusion between cells, viruses and cells, or transport vesicles and intracellular organelles employs distinct molecular machines.

1.1.2 Mitochondria membrane dynamics

Mitochondria undergo constant membrane fusion and fission events, leading to the mixing of membrane proteins and content. Fusion and fission are essential for normal mitochondrial function. Mitochondrial homotypic fusion is unusual because it involves the fusion of both outher and inner mitochondrial membranes with cognate partners (Martens and McMahon, 2008).

Mammals contain two mitofusins, Mfn1 and Mfn2, that localize to the mitochondrial outer membrane and cause aberrations in mitochondrial morphology when overexpressed. Mouse knockout studies have provided clear evidence that these proteins are essential for mitochondrial fusion. Mouse embryonic fibroblasts (MEFs) lacking either Mfn1 or Mfn2 have highly fragmented mitochondria in contrast to the tubular network observed in wild-type cells. Fusion assays indeed indicate a great reduction in the levels of mitochondrial fusion in single knockout MEFs and a complete loss of fusion in cells lacking both Mfn1 and Mfn2. Mfn1 and Mfn2 form homo-oligomeric and hetero-oligomeric complexes that are competent for fusion. Structural studies indicate that a heptad repeat region in the C-terminal portion of Mfn1 mediates oligomerization through an extended antiparallel coiled coil. This structure brings the opposing outer membranes to within approximately 100 Å of each other and thereby tethers mitochondria together during the fusion process. It is likely that subsequent conformational changes, perhaps driven by guanosine-5'-triphosphate **(**GTP) hydrolysis, are necessary to mediate membrane merger. When mitochondrial fusion rates are reduced, the mitochondrial population fragments into short tubules or small spheres because of ongoing mitochondrial fission in the face of less fusion. These observations support the idea that mitochondrial morphology is dictated by a balance between fusion and fission.

Human genetic studies identified OPA1 (Optic Atrophy 1) as the gene mutated in the most common form of dominant optic atrophy, a disease in which retinal ganglion cells degenerate and cause atrophy of the optic nerve. Depletion of OPA1 results in severe mitochondrial fragmentation that is due to loss of mitochondrial fusion. Along with the loss of mitochondrial fusion, OPA1 deficiency leads to other cellular defects, including reduction and disorganization of cristae membranes, severely reduced respiratory

capacity, and sensitivity to apoptosis. Unlike Mfn1 and Mfn2, OPA1 is not required on adjacent membranes for inner membrane fusion to proceed. OPA1 has a low intrinsic rate of GTP hydrolysis that is enhanced by assembly into a higher-order structure. Although it does not have an obvious pleckstrin homology (PH) domain, OPA1 is able to bind to lipid membranes that contain negatively charged phospholipids. In particular, OPA1 can bind to membranes containing cardiolipin, which is a signature lipid of the mitochondrial inner membrane. Upon binding to liposomes, OPA1 can deform the surface and cause the elaboration of lipid tubules. Mutations that are involved in dominant optic atrophy have been shown to disrupt GTP hydrolysis or lipid binding by OPA1 (Chan, 2012).

1.1.3 Proteins driving fission

Recent studies of protein-driven membrane rearrangements support the hypothesis that insertion of their amphipathic and small hydrophobic domains into the membrane matrix constitutes the major factor used by many proteins, including the BAR-domain proteins and dynamin family proteins, for membrane fission (Kozlov *et al.*, 2010).

1.1.4 Dynamin-1

For some fission processes, the formation of a membrane neck seems to involve membrane scaffolding by protein complexes. Membrane scaffolding also has been proposed for membrane fission driven by dynamin-1 (Kozlov *et al.*, 2010).

Dynamin is a large GTPase that has been shown to polymerize into a helical collar at the neck of endocytic buds, where it subsequently plays a key role in the formation of endocytic vesicles through fission. This function is fundamental, as the knockout of the dynamin neuronal isoform leads to striking defects in synapse organization and results in a strong dysfunction of neuronal activity. The recruitment of dynamin to endocytic buds is thought to depend on the local synthesis of phosphatidylinositol(4,5)bisphosphate (PIP2), as dynamin has a PIP2 binding pleckstrin homology (PH) domain.

Dynamin was one of the first proteins shown to tubulate protein-free charged liposomes. Because the final tubules are circled by dynamin helices, it is thought that dynamin polymerization provides the energy needed to deform the liposome membranes into a highly curved tubular structure (Roux *et al.*, 2010). The discovery of

dynamin self-assembly into helical structures on membrane surfaces and conformational changes of dynamin oligomers upon GTP hydrolysis have stimulated a series of mechanochemical models of dynamin action. These models propose that the formation of helical dynamin oligomers scaffolds the membrane into a cylindrical shape, which loses its stability and undergoes fission as a result of narrowing and/or stretching of the dynamin helix resulting from GTP hydrolysis and/or detachment of GDP-dynamin from the membrane surface.

1.1.5 BAR domain

The hydrophobic insertion mechanism assumes the partial embedding into the membrane matrix of hydrophobic or amphipatic protein domains. An integral trans-membrane domains spanning the whole membrane also bend membrane, if it had an assymmetric cone - or inverted cone- like shape or an oblique intra-membrane orientation. More biologically relevant appear to be small protein domains embedding only shallowly into the upper part of a lipid monolayer. Most frequently, such domains are represented by amphipathic alpha-helices, penetrating the membrane to the depth of about 40% of a monolayer thickness (Kozlov *et al.*, 2010).

BAR (Bin–Amphiphysin–Rvs) domains are modules that sense membrane curvature. This ability to bind preferentially to curved membranes can be deduced form the concave shape of the membrane-binding region. The sensing is shown by its tighter binding to liposome whose curvature is closer to the intrinsic curvature of the BAR. BAR domains are formed by dimerization, which is probably enhanced by membrane binding, and therefore the other consituent domain of the protein are presented in pairs. BAR domains are also frequently found in combination with N-terminal amphipatic helices (N-BAR domains). All these N-BAR domains lead to membrane tubulation *in vitro*.

In *Drosophila* the N-BAR protein amphipyhsin is involved in T-tubule formation in flight mucles and in its absence the T-tuble network is disrupted, preventing flight. In the synapse, amphipyhsin is proposed to form or stabilize a very different tubule structure.

The degree of positive curvature of the neck is close to that of the BAR, and thus this protein is suited for the recruitment of its binding partner, dynamin, to its correct location (McMahon and Gallop, 2005).

1.2 Endoplasmic reticulum

1.2.1 Endoplasmic reticulum shape

The endoplamsic reticulum (ER) has many different functions. These include the translocation of proteins (such as sectretory proteins) across the membrane; the integration of proteins into the membrane; the folding and modification of proteins in the ER lumen; the synthesis of phospholipids and steroids on the cytosolic side of the ER membrane; and the storage of calcium ions in the ER lumen and their regulated release into the cytosol (Voeltz *et al.*, 2002).

The interphase ER can be divided into nulear and peripheral ER. The nuclear ER, or nuclear envelope (NE), consists of two sheets of membranes with a lumen. The NE surrounds the nucleus, with the inner and the outher membranes connecting only at the nuclear pores. It is underlaid by a network of lamins. The peripheral ER is a network of interconnected tubules that extends througout the cell cytoplasm (Terasaki and Jaffe, 1991). The lumenal space of the peripheral ER is continuos with that of the nuclear envelope, and together they can comprise >10% of the total cell volume (Prinz *et al.*, 2000).

The ultrastructural of the ER has been visualized by electron microscopy in a number of cell types. The most obvious difference seen is between rough, i.e. ribosome-studded, and smooth region of the ER (RER and SER, respectively). The RER often has a tubular appearance, whereas the SER is often more dilatated and convoluted. The relative abundance of RER and SER found among different cell types correlates with their functions. For example, cells that secrete a large percentage of their synthesized proteins contain mostly RER (Voeltz *et al.*, 2002; Park and Blackstone, 2010).

1.2.2 The ER is a single compartment

Several approaches have provided evidence that the ER is a single membrane system with a continuous intralumenal space. In one experiment, a fluorescent dye that cannot exchange between discontinuous membranes was injected into cells in an oil droplet. The dye diffused throughout the cell in a membrane network that, based on morphological criteria, was the ER. This was observed in a number of different cell types including sea urchin eggs (Terasaki and Jaffe, 1991) and Purkinje neurons (Terasaki *et al.*, 1994). Because the dye spread in fixed as well as live cells it must be

diffusing through a continuous network rather than being transported by active trafficking.

The continuity of ER membranes network was also proved by fluorescence loss in photobleaching (FLIP). In this experiment, GFP-tagged proteins are targeted either to the lumen or membrane of the organelle, and then a small region of the labeled membrane is continuously bleached using the beam from a confocal laser scanning microscope. If membranes are interconnected, unbleached fluorescent molecules diffuse into the illuminated spot, where they are bleached; eventually, the fluorescence of the entire organelle is depleted. When FLIP experiments were performed on ER membranes, all fluorescence was rapidly lost from the entire membrane network (Dayel and Verkman, 1999), indicating the continuity of the ER membrane system.

1.2.3 Propagation of ER during cell division

All components of the cell are dramatically rearranged during cell division. Accumulating evidence suggests that the ER network does not disassemble into vesicles during the cell cycle, but that it is divided between daughter cells by cytokinesis. The strongest support for maintenance of ER continuity comes from FLIP experiments demonstrating that ER markers retain interphase patterns of motility during mitosis (Ellenberg *et al.*, 1997). In addition, both light and electron microscopy show that ER networks can be visualized during cell division (Koch and Booth, 1988; Ellenberg *et al.*, 1997; Terasaki, 2000).

The NE disassembles during mitosis in most eukaryotic cells: the scaffolds to which NE membrane proteins are bound in interphase are reorganized, the lamina is disassembled and the chromatin is condensed. In addition, phosphorylation of many NE proteins reduces their affinity for these partners and imaging of these proteins suggests that once freed, they diffuse throughout the ER network (Collas and Courvalin, 2000). However, biochemical fractionation of mitotic or meiotic cells has shown that vesicles are enriched in NE proteins, particularly in egg cells (Gant and Wilson, 1997). It is not clear whether this result reflects a portion of the ER that maintains a distinct composition because it is not part of the bulk ER network, or whether domains are somehow retained in the absence of scaffolds like the lamina.

1.2.4 Dynamics of the ER

In interphase cells, the peripheral ER is a dynamic network consisting of cisternal sheets, linear tubules, polygonal reticulum and three-way junctions (Allan and Vale, 1991). Several basic movements contribute to its dynamics: elongation and retraction of tubules, tubule branching, sliding of tubule junctions and the disappearance of polygons. These movements are constantly rearranging the ER network while maintaining its characteristic structure. Although continuous shape changes are seen consistently, the relationship between ER dynamics and ER functions remains still unclear.

Different mechanisms underlie the different modalities of ER dynamics. The dynamics of the ER network depend on the cytoskeleton. In mammalian tissue culture cells, goldfish scale cells, and *Xenopus* and sea urchin embryos the ER tubules often co-align with microtubules. Microtubule-based ER dynamics were studied with time-lapse microscopy and appear to be based on three different mechanisms. First, new ER tubules can be pulled out of existing tubules by motor proteins migrating along microtubules. CLIMP63, a resident ER membrane protein that contains a MT binding domain and is excluded from the nuclear envelope, has been propose to provide a direct link between MTs and the ER thus helping to distribute the ER in the cytoplasm. Secondly, new tubules may be dragged along by the tips of polymerizing microtubules. There are two distinct mechanisms whereby ER tubules move along MTs. One mechanism is defined as tip attachment complex (TAC) dynamics and involves the attachment of the tip of the ER tubule to the tip of the MT plus end. The second mechanism is defined as sliding and involves binding of the tip of the ER tubule to an extending MT shaft followed by sliding of the ER tubule along the MT. ER tubule sliding is faster and more frequent than TAC dynamics but the proteins that mediate this process have not yet identified. Recently, it has been shown that ER sliding occurs on stable MTs post-translationally modified by acetylation. Finally, ER tubules may associate with the sides of microtubules, via motor proteins, as they slide along other microtubules. Each of these mechanisms can lead to tubule extension and, when tubules intersect, they fuse and create three-way junctions (Voeltz *et al.*, 2002; Waterman-Storer and Salmon, 1998).

In yeast and plants, the actin cytoskeleton, rather than the microtubule network, is required for ER dynamics (Prinz *et al.*, 2000).

The cytoskeleton contributes to ER dynamics, but it is not necessary for the maintenance of the existing ER network. Although depolymerization of microtubules by nocodazole in mammalian tissue culture cells inhibits new tubule growth and causes some retraction of ER tubules from the cell periphery, the basic tubular-cisternal structure of the ER remains intact (Terasaki *et al.,* 1986). Similarly, actin depolymerization in yeast blocks ER movements but does not disrupt its structure (Prinz *et al.,* 2000).

A complex interplay of factors is likely to ultimately determine membrane morphology, however, another important way to shape membranes involves the use of proteins endowed with the ability to deform lipid bilayers (Zimmerberg and Kozlov, 2006). Proteins can shape membranes in a variety of ways. Mechanical force can be applied to a lipid bilayer by molecular motors pulling on membrane proteins. Peripheral membrane proteins with an intrinsic curvature can conform membranes to their shape, and integral membrane proteins with specialized hydrophobic domains can selectively insert or wedge into the outer monolayer to physically generate curvature (Pendin *et al.*, 2011).

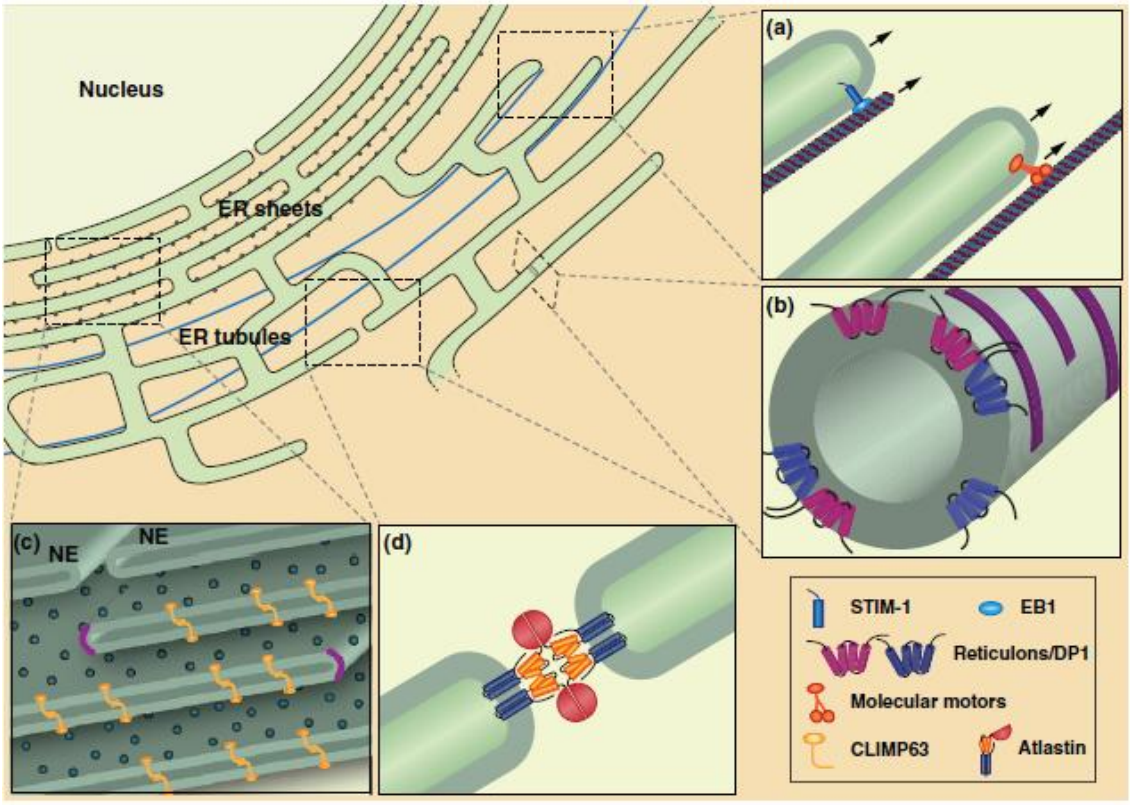

Fig.1 Domain organization of the endoplasmic reticulum network within the cell
(a) ER tubules move about the cytoplasm by attaching to microtubules using a TAC mechanism (left) or by a sliding mechanism (right). (b) the reticulons and Dp1/REEP/Yop1 shape flat membranes into tubules using a combined wedging and scaffolding mechanism. Their hydrophobic segments insert like a wedge in the outer lipid layer causing the bilayer to bend and their ability to homo- and hetero-oligomerize may produce arc-like scaffolds around the tubules. (c) ER sheets, observed here in cross section, can be generated by the presence of the reticulons and Dp1/REEP/Yop1 at their edges to stabilize locally the high curvature. In addition, transmembrane scaffolding proteins localized in both membranes interact through their luminal domains to maintain the two membranes flat and at a constant distance. NE, nuclear envelope. (d) two ER tubules in the process of being merged by the fusogenic activity of the atlastin GTPase (Pendin *et al.*, 2011).

1.3 Atlastin

1.3.1 SPG3A gene

Hereditary spastic paraplegias (HSPs) are a group of genetically heterogeneous neurological disorders, characterized by progressive spasticity and weakness of the lower limbs that are caused by degeneration, or failure to develop, of the corticospinal tract. Mutation in the SPG3A gene on chromosome 14 were identified for the first in HSP patients in 2001 and cause the most frequent autosomal dominant form of pure HSP with very early onset and the second most frequent of all autosomal dominant form of this disease. The gene encodes a 558 aminoacid protein, atlastin, a new member of the dynamin superfamily of large GTPases, (Namekawa *et al.*, 2007).

So far, 38 mutations have been reported in atlastin-1, most of which cause early-onset pure autosomal-dominant HSP by haploinsufficiency (Fassier *et al.*, 2010).
Atlastin protein is prominently enriched in the lamina V pyramidal neurons in the cerebral cortex, a subpopulation of which exhibit a distal axonopathy in patients with SPG3A. These upper motor neurons project to lower motor neurons in the lumbar spinal cord, and their dysfunction results in a spastic paraparesis, the cardinal feature of HSPs. Because these neurons have among the longest axons in the central nervous system, their dysfunction in SPG3A patients may reflect a critical role for proper atlastin-1 function in this sub-population of "long axon" upper motor neurons (Zhu *et al.*, 2003).

1.3.2 Atlastin family

There are two higly related human proteins similar to atlastin (renamed atlastin-1): atlastin-2 and atlastin-3. These proteins show extensive homology, with a large central core of higher similarity that includes the GTP-binding region in the N-terminal portion; the most divergence occurs at the C and N termini. There is 69% aminoacid identity and 79% similarity between atlastin-1 and atlastin-2 over the central 533 residues and 66% identity and 75% similarity between atlastin-1 and atlastin-3 over 476 residues. Atlastin-2 and atlastin-3 share 67% identity and 78% similarity over 482 residues. Also, two predicted transmembrane helices are conserved in all three proteins (Zhu *et al.*, 2003).

1.3.3 Human atlastin localization and function

The cellular function of atlastin is still unknown. Although atlastin proteins are highly similar structurally, their distributions among tissues vary substantially (Rismanchi *et al.*, 2008). While atlastin-2 and -3 are localized to the ER, endogenous atlastin-1 has been reported to localise to the cis-Golgi in neurons. Moreover, atlastin-1 has been reported to be mainly expressed in the brain and, at much lower levels in lung, smooth muscle, adrenal gland, kidney, and testis (Zhu *et al.*, 2003), while atlastin-2 and -3 are ubiquitously expressed (Farhan and Hauri, 2009).
Small interfering RNA-mediated knockdown of atlastin-2 or -3 results in a normal ER morphology under fluorescence microscopy, with a small subset of double-knockdown cells showing a more tubular, less reticular ER. The most pronounced effect of atlastin reduction is on Golgi morphology (Rismanchi *et al.*, 2008). The Golgi in atlastin-2 or -3

knockdown cells was fragmented, resembling mini-stacks or elongated tubules, but protein trafficking was normal. The reason for the dramatic change in Golgi morphology and a relatively minor effect on ER structure remains obscure. These morphological changes might be an indirect result of altered communication between the ER and subsequent secretory compartments that is not reflected in bulk protein traffic.

Overexpression of wild-type atlastin-1 resulted in the formation of aberrant sheet-like structures; instead overexpression of wild-type atlastin-2 or -3 did not noticeably affect ER morphology as seen by light microscopy, but produced a fragmented Golgi. However, overexpression of GTPase-deficient mutants of atlastin-1-3 resulted in more elongated and tubular ER with less branching, as well as a fragmented Golgi. These effects might be a result of a dominant-negative effect of the overexpressed protein. Overexpression of either wild-type or mutant atlastins did not significantly affect protein trafficking (Rismanchi *et al.*, 2008; Farhan and Hauri, 2009).

The effects of atlastin reduction were also examined in neurons, the primary site of action for HSP. Atlastin-1 knockdown in primary rat cerebral cortical neurons showed reduced axonal length, an increased number of neurons without axons, and a reduced number of dendrites per cell (Zhu *et al.*, 2006). It is possible that specific ER functions such as appropriate calcium homeostasis are required for proper neurite outgrowth or axonal pathfinding, and that these functions are disrupted when atlastin-mediated fusion is lost.

Atlastin has been shown to interact with spastin, a microtubule severing protein responsible for the autosomal dominant HSP SPG4 but there is conflicting evidence with regard to the interacting regions. In one case, the N-terminal 80 amino acids of spastin were required for an interaction with the N-terminal cytoplasmic domain of atlastin-1. In another series of experiments, the C terminus of atlastin-1 was required for an interaction with full-length spastin, suggesting a mutually exclusive region of atlastin-1 required for spastin interaction (Moss *et al.*, 2011).

Most recently, an association between three HSP-related proteins, atlastin, spastin and receptor accessory protein 1 (REEP1), was reported (Park *et al.*, 2010). This work showed that the interaction between atlastin and REEP1 probably occurs through hydrophobic membrane-spanning domains in each protein, similar to the interaction of atlastin with other reticulons (Hu *et al.*, 2009). This recent study also reported that the interaction between spastin and atlastin required the N-terminal transmembrane

segment of the M1 isoform of spastin and the two tandem TMDs of atlastin. Additionally, spastin interaction with atlastin is limited to atlastin-1, because atlastin-2 and atlastin-3 do not appear to interact with spastin (Rismanchi *et al.*, 2008).

In 2009, a liposome assay showed that atlastin-1 was able to tubulate and vesiculate simple liposome membranes like dynamin: purified atlastin could produce vesicles from artificial protein-free membranes: liposomes in the presence of GTP or GTPgammaS induced formation of tubules resembling those induced by dynamin and mimicking the three-way junctions that characterized the ER structure. However, another predominant phenotype, as well as the tubule formation, was a profuse vesicle formation. This secondary, but not less frequent phenotype, may be due to the composition of liposomes that was reported to influence the protein propensity to form tubules or vesicles (Muriel *et al.*, 2009). Therefore, until now, there is no clear evidence that human atlastins, like their *Drosophila* homolog are able to fuse homotipically the ER membranes.

A recent study examined the consequences of altering atlastin-1 levels in the zebrafish *Danio rerio* by morpholino-mediated knockdown and overexpression (Fassier *et al.*, 2010). Decreased levels of atlastin-1 resulted in aberrant spinal motor axons, which caused a reduction in larval movement. Molecular analysis indicated that bone morphogenic protein (BMP) signaling was upregulated in the knockdown and inhibited by atlastin-1 overexpression, suggesting a role in receptor trafficking. It has been shown also that atlastin-1 localizes to endosomes, and its deletion did not affect ER structure when examined under fluorescence microscopy.

1.3.4 Atlastin structure

Recently, two groups have solved the X-ray crystal structure of the soluble domain (1-446) of human atlastin-1 (Bian *et al.*, 2011; Byrnes and Sondermann, 2011). The structures reveal a globular GTPase head connected through an eight–amino acid linker to a middle domain comprised of a three-helix bundle. The GTPase domain has an overall fold similar to that of GBP1, the closest relative of atlastin1-3 in the dynamin superfamily.

Dynamin superfamily members undergo conformational changes in a manner dependent on their nucleotide-bound state. Accordingly, atlastin-1 crystallization by both groups was performed in the presence of a variety of GTP analogues. Both groups observed two strikingly distinct atlastin-1 conformers, indicating that, like GBP1 and dynamin, atlastin-1 indeed undergoes discrete conformational changes during its reaction cycle.

Moreover, both structures showed atlastin-1 as a head to head dimer, reminiscent of the head to head dimers observed in crystal structures of the GTPase domains of dynamin bound to the transition state analogue GDP + aluminum fluoride (Chappie *et al.*, 2010).
The dimer pairs suggest a compelling model for membrane tethering and fusion. Head to head dimerization of atlastin in trans would initiate membrane tethering. Once tethered, crossover of the middle domains would catalyze membrane fusion, presumably by bringing opposing lipid bilayers into tight apposition and deforming them, consequently reducing the activation barrier for membrane fusion. In part because dimerization of atlastin in solution is nucleotide dependent, GTP binding has been suggested to form the prefusion dimer for the membrane-tethering step, whereas GTP hydrolysis and Pi release has been hypothesized to trigger the 90° rotation and crossover of the middle domains to achieve the fused state. According to this scenario, a cycle of GTP binding and hydrolysis would drive both membrane tethering and fusion, though how the postfusion complex is disassembled for further rounds of fusion remains to be clarified. If the crossed dimer conformation indeed represents the postfusion state, contacts unique to this conformer should be important for driving membrane fusion. Conversely, inhibiting such contacts should block the conversion of prefusion dimers to the postfusion state (Morin-Leisk *et al.*, 2011).
Computational structural modeling of atlastin-2 based on its similarity to GBP1 have revealed an intramolecular salt bridge required for the ER network branching function of atlastin-2. The ionic interaction between the lysine in position 372 and the aminoacid in position 380, an aspartic acid (K372-E380) is important for atlastin function and is likely caused by its stabilization of the postfusion dimer conformation. Based on the position of the salt bridge in the context of the postfusion dimer, it is possibly that the ionic contact constrains the linker in a kinked conformation relative to the head and middle domains. In so doing, it may serve to position other two intervening nonpolar residues (M374 and L375) that need to pack extensively against the opposing head, to form the postfusion conformation. In the absence of the salt bridge, the linker may be rendered too flexible, reducing the ability of these nonpolar residues to pack effectively (Morin-Leisk *et al.*, 2011).
It remains to be clarified how changes in the nucleotide-bound state of atlastin-1 relate to changes in its conformation.

1.3.5 *Drosophila* atlastin

The *Drosophila* genome produces a single atlastin protein that is 541 amino acids in length. The *Drosophila* atlastin (atl) sequence is strongly homologous with all three human isoforms, with 44–49% identity (61–68% similarity) over the entire length of the protein (Moss *et al.*, 2011).

Drosophila and human atlastins show remarkable homology and conservation of domain organization. Immunohistochemistry experiments showed that *Drosophila* atlastin is ubiquitously expressed, and its expression levels are high during embryonic development.

In vivo and *in vitro* analysis provides strong evidence that *Drosophila* atlastin is the vital GTPase required for homotypic fusion of ER membranes. In response to loss of atlastin, the ER network becomes fragmented but no obvious transport impairment was observed, supporting a function in the maintenance of ER integrity rather than in secretory traffic. Nevertheless, suitable transport defects after fragmentation cannot be completely ruled out.

Drosophila atlastin is capable of homo-oligomerization and self-association can occur within the same membrane as well as between opposing membranes. This property leads to the formation of trans-complexes that tether adjacent ER membranes. *In vivo* overexpression of atlastin results in the expansion of ER elements, consistent with excessive membrane fusion. In agreement with *in vivo* experiments, recombinant atlastin potently drives membrane fusion *in vitro* in a GTP-dependent manner. Atlastin requires GTPase activity to exert its function because GTPase-deficient atlastin (K51A) is functionally inactive *in vivo*, fails to tether ER membranes owing to its inability to homo-oligomerize, and does not promote membrane fusion *in vitro* (Orso *et al.*, 2009).

The structure of the N-terminal cytoplasmic domain (residues 1-446) of human atlastin-1 was solved by X-ray crystallography in two recent studies. Molecular modeling approach indicates that the N-terminal cytosolic region of *Drosophila* atlastin is highly likely to adopt a conformation similar to that observed for atlastin-1. In particular, the middle region contains the predicted α-helix and its sequence is compatible with folding as a three-helix bundle (Pendin *et al.*, 2011).

The structure-function studies of *Drosophila* atlastin have led to develop a working model of atlastin function in membrane fusion. The fusion cycle begins with nucleotide-free atlastin monomers in opposing ER membranes. Then the nucleotide binding results

in a permissive state for association between the GTPase domains. The interaction between GTPase domains matures to a more stable dimer facilitated primarily by an interaction between the middle domain three-helical bundle segments. This conformational change is achieved, perhaps driven by nucleotide hydrolysis, by rotating the GTPase domain dimer 180 degrees which forces the three-helix bundles into close proximity. The new association between adjacent 3HBs liberates the C-terminal tail domain to perform its required role. The activity of this C-terminal domain may be accomplished by forming a new association with the dimeric 3HB or by direct interaction with lipid. We currently favor a direct interaction with lipid based on the amphipathic nature of this protein sequence. An interaction between the membrane surface and the amphipathic C-terminal tail could destabilize the bilayer and provide the driving force for outer leaflet mixing, resulting in a hemifusion intermediate that resolves by inner leaflet mixing to full fusion. Finally, the GDP release could then promote dissociation (Moss *et al.*, 2011).

It is also possible that an interaction between the 3HBs of opposing atlastin molecules occurs during the nucleotide-dependent conformational change. It seems that the 3HB plays a minor or negligible role in the nucleotide-indipendent oligomerization of atlastin molecules, rather, the trans-membranes mediate this association of atlastin molecules in the same membrane before nucleotide binding (Liu *et al.*, 2012).

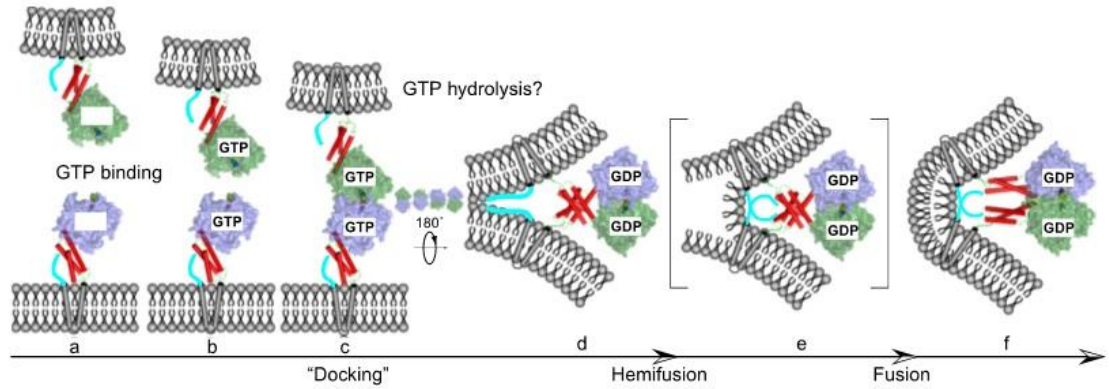

Fig. 2 Model for atlastin-mediated fusion

The GTPase domains are cartooned as surface representations, the middle domains are shown as red cylinders, the transmembrane domains are illustrated as gray cylinders, and the C-terminal tails are shown as thick cyan lines. (a) Bilayer containing nucleotide-free prefusion monomers. (b) GTP-bound prefusion monomers. (c) Initial, unstable docking intermediate between GTP-bound monomers through surfaces on the GTPase domain. (d) Stabilized dimer formed by domain rotation and 3HB interaction resulting from GTP hydrolysis. (e) Putative hemifusion intermediate. (f) Postfusion bilayer (Moss *et al.*, 2011).

1.4 Reticulon and DP1

1.4.1 Reticulon and DP1 family

Reticulons (RTNs) have been identified in the genomes of *Homo sapiens*, *Mus musculus*, *Danio rerio*, *Xenopus laevis*, *Drosophila melanogaster*, *Caenorhabditis elegans*, *Arabidopsis thaliana*, *Saccharomyces cerevisiae* and many other eukaryotes, but not in archaea or bacteria. In mammals, there are four RTN genes encoding RTN proteins RTN1-4. The reticulons homology domains of RTN1, 3 and 4 share the highest sequence identity at the aminoacid level (average 73%), whereas RTN2 has only 52% identity with human RTN4 (Yang and Strittmatter, 2007).

Mutation in RTN2 (codified by SPG12), like insertion, deletion and substitution, are associated with autosomal dominant uncomplicated HSP (Montenegro *et al.*, 2012) while missense mutation in RTN4 are implicated in schizophrenia (Lazar *et al.*, 2011).

The other family consists of the DP1/Yop1p proteins, which includes six mammalian *DP1/REEP* genes and the yeast ortholog Yop1 (Hu *et al.*, 2008; Hu *et al.*, 2009).

1.4.2 Reticulon and DP1: structure and localization

Reticulons do not share any primary sequence homology with members of the DP1/Yop1p family. However, both families have a conserved domain of 200 amino acids containing two long hydrophobic segments (Shibata *et al.*, 2008). The RHD (Reticulon Homology Domain) consists of two hydrophobic regions, each 28-36 amino acids long, which are thought to be membrane-embedded regions, separated by a hydrophilic loop of 60-70 amino acids, and followed by a carboxy-terminal tail about 50 amino acids long. Although much amino-acid identity has been lost over the course of evolution, the overall structure of the RHD has been preserved from plants to yeasts to humans. This suggests that three-dimensional protein structure is of greater importance than individual residues for RHD function. The RHD hydrophobic regions are unusually long for transmembrane domains: each spans approximately 30-35 amino acids, whereas most transmembrane domains are about 20 amino acids in length. This raises the interesting question of whether this longer length has significance for RTN function. Each hydrophobic segment seems to form, in reticulon and DP1, a hairpin within the lipid bilayer so that all hydrophilic segments are found in the cytoplasm (Shibata *et al.*, 2008).

This particular RHD length is a required domain for DP1 and reticulon partitioning and interactioning in the ER membrane. Using fluorescence recovery after photobleaching, it has been revealed that mammalian reticulons and DP1, like their yeast homolog, are less mobile in the membrane than normal ER proteins. This slow diffusion is probably not caused by their tethering to the cytoskeleton. Rather, immobility appears to be caused by their oligomerization that is evident in sucrose gradient centrifugation and cross-linking experiments. The conserved RHD containing the two hydrophobic segments is sufficient for RTN oligomerization. This conclusion is supported by the isolation of mutants of yeast Rtn1p that have amino acid changes in the RHD; they oligomerize less extensively according to sucrose gradient sedimentation experiments, and they diffuse rapidly in the membrane. The same mutants also no longer localize exclusively to the tubular ER, suggesting that oligomerization of the RTNs and DP1/Yop1p is required for their proper localization. Regulation of RTN oligomerization may have physiological consequences as well. It has recently been shown that over-expression of one reticulon isoform in mice leads to large SDS-resistant oligomers in neurons, and these mice exhibit neuropathies similar to that of Alzheimer disease (Shibata *et al.*, 2008).

The amino-terminal regions of different RTNs are highly divergent in sequence. The amino-terminal domains of the human RTN4 isoforms appear to be highly unstructured, even under physiological conditions. Recent studies have shown that intrinsically unstructured proteins (IUPs) are more likely to form multiprotein complexes than are proteins with stable tertiary structure, are better able to ‘moonlight’ - carry out alternative functions - and may fold upon binding to their partners. The characterization of RTN4 as an intrinsically unstructured/disordered protein may explain its involvement in many physiological processes (Yang and Strittmatter, 2007).

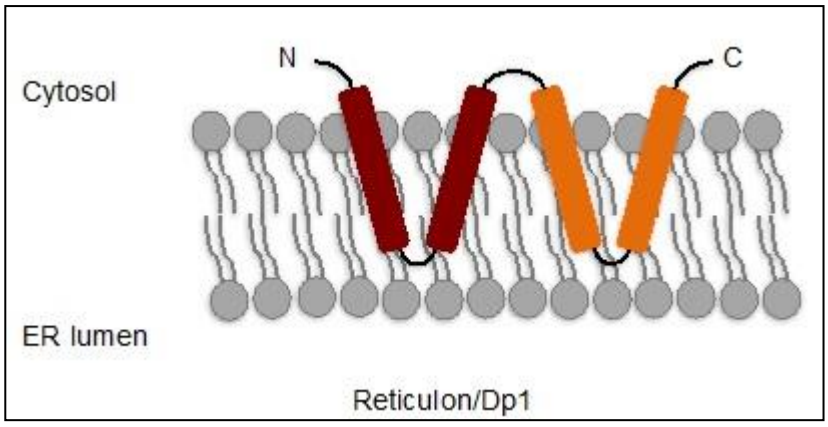

Fig. 3 Reticulon and DP1 structure
Reticulon and DP1 proteins contain large hydrophobic segments that are longer than conventional α-helical transmembrane domains. Zurek *et al.* (2011) and Voeltz *et al.* (2006) provide data suggesting that these domains adopt a hairpin conformation when inserted into the lipid bilayer. This topology results in the bulk of the hydrophobic portion of the protein being preferentially located in the outer leaflet of the lipid bilayer. The net result is that the protein has a "wedge shaped" envelope and its insertion into a lipid bilayer might create membrane curvature by providing more bulk in the outer leaflet (Collins, 2006).

1.4.3 Reticulon and DP1 protein function

The first known RTN protein, RTN1, was identified from a cDNA in neural tissue and subsequently characterized as an antigen specific to neuroendocrine cells. This so-called neuroendocrine-specific protein (NSP) was later renamed RTN when it was discovered to be associated with the ER in COS-1 cells. RTNs do not contain an ER localization sequence per se, but a single RHD hydrophobic region is sufficient to target the protein to the ER.

Most RTN research has focused on RTN4 in the central nervous system and its effects on neurite outgrowth and axonal regeneration after spinal cord injury. However, the presence of RTNs in all eukaryotic organisms and their ubiquitous ER-associated expression indicate a more general role. Until now there are three areas of RTN localization and function: ER-associated roles, oligodendrocyte-associated roles in inhibition of neurite outgrowth, and the role of RTNs in neurodegenerative diseases (Yang and Stritmatter, 2007).

RTN3 (and other RTNs) appear to interact with BACE1, the beta-secretase enzyme responsible for amiloidogenic processing of the amyloid precursor protein (APP) to generate amyloid beta. Overexpression of all RTNs 1-4 reduces amyloid beta production. The mechanistic basis of how RTN3 and other RTNs may function as a negative modulator of amyloid beta production is unclear. RTN3-BACE1 association

may directly affect the latter's enzymatic activity, but another possibility is that the association of RTN 3 and BACE1 alters its trafficking itinerary. APP and BACE1 have similar trafficking itineraries in the exocytic end endocytic pathways.

Both reticulon and DP1 proteins are ubiquitously expressed in all eukaryotes and localize predominantly to the tubular ER (Voeltz *et al.*, 2006). Their overexpression renders the mammalian ER network resistant to the rearrangement that follows microtubule depolymerization (Shibata *et al.*, 2008), and overexpression of certain reticulon isoforms leads to long and unbranched tubules (Hu *et al.*, 2009).

Reticulons may also have a role in shaping the endoplasmic reticulum under certain stress condition. Infact, there is evidence for transient overexpression of very high levels of RTNs inducing ER stress and apoptosis, but a more moderate and sustained expression may not lead to cell death, and could infact precondition cells against further stress (Teng and Tang, 2008).

1.4.4 Reticulon in plant

Very little is known about the function of RTN proteins in plants. The *Arabidopsis thaliana* genome contains at least 19 closely related RTN-like proteins, 15 of which have been annotated. RTNs show great variability in their N-terminal domains, which are involved in a wide variety of interactions. As there is virtually no functional information available about the role of RTNs in plant cells, it has been selected, for all research studies, the isoforms with the shortest N-terminal domain, RTNLB13, which comprises an intact RHD flanked by very short N- and C-terminal regions. Overexpression of RTNLB13 in tobacco leaf epidermal cells by *Agrobacterium* infiltration altered dramatically the appearance of the cortical ER: the ER tubules were no longer detectable and were replaced by clusters of large vesicle-like structures. Although, RTN-induced ER morphology alteration has no major effect on the anterograde secretory pathway (Tolley *et al.*, 2008).

Accordingly to the yeast and mammalian experiments, full-length TMDs are necessary for the ability of RTNLB13 to reside in the ER membrane and to form low-mobility complexes within the ER membrane (Tolley *et al.*, 2010).

1.4.5 *Drosophila* reticulon

Drosophila reticulon was discovered in a screen to identify proteins enriched in axons of the developing *Drosophila* embryonic nervous system. *Drosophila* Rtnl1 (Reticulon-like 1) bears no closer resemblance to RTN1, RTN3 or RTN4/Nogo, but is more similar to this group than it is to RTN2.

The gene is transcribed from seven promoters producing seven transcripts, which encode five different polypeptides. Each of these transcripts includes at their 3' end the four C-terminal exons that encode the RHD. There are experimental evidence that Rtnl1 is the only RTN that is normally expressed by *Drosophila*. An additional RTN-like sequence is also present in the *Drosophila* genome, Rtnl2, which is more similar to RTN2 but this is possibly a retronuon with pseudogene character. Rtnl2 has a genomic organization very distinct from other members of the reticulon family as it bears a single intron within its RHD-containing exons. Unlike Rtnl1, for which there are greater than 150 ESTs, there are only four ESTs identified for Rtnl2, all of which originate from animals that have been challenged with bacteria. Indeed there is no detectable expression of Rtnl2 transcripts in the wild-type animal using *in situ* hybridization.

In contrast, the Rtnl1 protein is expressed ubiquitously in the embryo and shows increased expression within the nervous system at later stages of embryogenesis. The protein continues to be expressed throughout the animal in post-embryonic stages where it is retained within the nervous system with expression extending throughout axons and at presynaptic specializations. This enrichment within the nervous system is characteristic of RTNs identified in other species (Wakefield and Tear, 2006). Expression of Rtnl1 is also found in muscles and, at subcellular level, Rtnl1 localizes to ER membranes.

Recent studies have characterized a *Drosophila* model of HSP caused by loss of the human orthologue of SPG12, Rtnl1. The loss of Rtnl1 led to an expansion of the rough or sheet ER in larval epidermis and elevated levels of ER stress. It also caused abnormalities specifically within the distal portion of longer motor axons and in their presynaptic terminals, including disruption of the smooth ER, the microtubule cytoskeleton and mitochondria. This is the first animal model providing evidence of an ER phenotype due to the loss of RTN and shows that major arrangements of ER morphology do not noticeably affect organism survival (O'Sullivan *et al.*, 2012).

1.5 *Drosophila melanogaster* as model organism

Drosophila melanogaster has provided powerful genetic system in which to elucidate fundamental cellular pathways in the context of a developing and functioning nervous system. *Drosophila* allows study of the normal function of disease proteins, as well as study of effects of familial mutations upon targeted expression of human mutant form in flies. These studies have revealed new insight into the normal function of such disease proteins, as well as provided models in *Drosophila* that will allow genetic approaches to be applied toward elucidating ways to prevent or delay toxic effects of such disease proteins (Chan and Bonini, 2000).

Modeling human brain disease in *Drosophila melanogaster* offers several advantages (Jeibmann and Paulus, 2009). The first and foremost reason why flies are exploited as models of human diseases is based on the presumption that fundamental aspects of cell biology relevant to processes as diverse as cell cycle regulation, synaptogenesis, membrane trafficking, and cell death are similar in *Drosophila* and humans (Jackson, 2008). A report demonstrating that approximately 75% of the disease-related loci in humans have at least one *Drosophila* homologue cements this high degree of conservation present in flies.

Furthermore, studies of developmental events in the fly and subsequent similar studies in higher animals have revealed a stunning degree of functional conservation of genes. Indeed, the fly brain is estimated to have, strikingly enough, in excess of 300,000 neurons and similarly to mammals is organized into areas with separated specialized functions such as learning, memory, olfaction and vision.

Drosophila has an unrivalled battery of genetic tools including a rapidly expanding collection of mutants, transposon-based methods for gene manipulation and systems that allow controlled ectopic gene expression and balancer chromosomes (Cauchi and van den Heuvel, 2006). It should be possible to target endogenous wild-type copies of "disease gene" in the fly genome for inactivation (knock-out); defined mutations can also be "engineered" (knock-in) into respective endogenous genes, to create gain-of-function models (Chan and Bonini, 2000).

The above characteristics of such a minuscule system model, combined with the rapid generation time, inexpensive culture requirements, large progeny numbers produced in

a single cross and a small highly annotated genome devoid of genetic redundancy, are poised to yield seminal insights into human disease (Cauchi and van den Heuvel, 2006). For almost a century, fruit flies have been providing a useful toll to study various different subjects: form the chemical basis of mutagenesis, to the definition of genes, from developmental biology, to animal behaviour. The ability to use *Drosophila* as a powerful tool to approach pathogenetic disease mechanisms for human diseases speaks to a tremendous application in biomedical research (Chan and Bonini, 2000).

2 METHODS

2.1 Molecular biology

The atlastin full-length complementary DNA was previously obtained by RT-PCR performed on total *Drosophila* RNA. The cDNA was cloned in pcDNA3.1Zeo+ vector in frame with a Myc or HA tag sequence. The atlastin/pcDNA3.1Zeo+ construct used for the experiments has been previously generated.

2.1.1 Cloning of truncated 1-422, 1-471 and 1-497 *Drosophila* atlastin (atl) cDNA in pcDNA3.1 Zeo+ plasmid

pcDNA3.1Zeo+ is a plasmid designed for high level expression in a variety of mammalian cell lines (Appendix C).

Three atlastin fragments were cloned in pcDNA3.1Zeo+ plasmid: atl(1-422) encompassing the GTP binding domain and the 3-helix buldle, atl(1-471) and atl(1-497) that lackes entirely or the last 70 aminoacids of the C-terminal cytoplasmatic tail, respectively.

A Myc-tagged versions of each truncated atlastin were cloned in the pcDNA3.1Zeo+ plasmid. To insert the Myc epitope in the C-terminus of *Drosophila* atlastin, cDNA was amplified from wild-type atl/pcDNA3.1Zeo+ using the following primers:

Atl ATG EcoRI F

5’AGCTGAATTCATGGGCGGATGGGCAGTGCAGG3’

Atl422 Myc XhoI R

5’AGCTCTCGAGCTACAGATCTTCTTCAGAAATAAGTTTTTGTTCTGTCCGTG CTGCCTTAAAGATG3’

Atl471 Myc XhoI R

5’AGCTCTCGAGCTACAGATCTTCTTCAGAAATAAGTTTTTGTTCATATCTAA TGTAGGCCCACAG3’

Atl497 Myc XhoI R

5’AGCTCTCGAGCTACAGATCTTCTTCAGAAATAAGTTTTTGTTCGATGGGTC GCATGAATTTCTC3’

PCR reaction

atl/pcDNA3.1Zeo+ template	50 ng
Forward (10 uM)	2 ul
Reverse (10 uM)	2 ul
10 mM dNTPs	1 ul
5X Phusion HF buffer	10 ul
Phusion DNA polymerase	2.5U
H2O	to 50 ul

PCR cycle

98°C 30 seconds

98°C 10 seconds
57°C 20 seconds
72°C 1 minute
} 30 cycles

72°C 10 minutes

Restriction reactions

2 ug of pcDNA3.1Zeo+ plasmid and PCR fragments were digested using 20 U of EcoRI and XhoI restriction enzymes. Mixed products were incubated at 37°C for 1 hour and successively separated by electrophoresis in a 1% agarose gel. The bands corresponding to the atl PCR fragments and pcDNA3.1Zeo+ plasmid were cut from gel and purified using the QIAquick Gel Extraction Kit (Qiagen). Purified DNA products were eluted in 20 ul of elution buffer. The purified DNA fragments were ligated as follows:

pcDNA3.1Zeo+	150 ng
atl fragment	300 ng
10X Ligation buffer	1 ul
T4 DNA ligase (Biolabs)	1 ul
H2O	to 10 ul

The mixture was incubated at room temperature for 1 hour.

Transformation

Ligation mixture was used for transformation of chemically competent DH5alpha cells (Invitogen). Transformed bacteria were plated on LB–ampicillin agar plates and incubated overnight at 37°C. Five colonies for each construct were grown in LB medium with ampicillin. Plasmid DNA was successively purified by minipreparation protocol (Appendix A) and tested by restriction analysis.

Purification of Myc-tagged atl(1-422), atl(1-471), and atl(1-497) in pcDNA3.1Zeo+

Plasmid DNA was purified from an overnight culture using a "Midi" plasmid purification kit, according to NucleoBond Xtra Midi purification protocols (Macherey-Nagel). The final pellets were re-suspended in 50 ul of TE buffer.

All the steps, starting from PCR reaction to transformation and purification, are common to all the constructs generated. For the preparation of the following constructs, it will indicate only the primers designed and the restriction site used. The PCR cycle will adjust accordingly to the annealing temperature of the primers and the time of extension accordingly to the length of the fragment amplified.

2.1.2 Generation of atlastin(1xlinker) and atlastin(3xlinker) in pcDNA3.1Zeo+ plasmid

Between the 3-helix bundle domain and the first transmembrane domain of atlastin protein there are five aminoacids.
To generate linker insertion mutants a unique SacII site was introduced in the juxtamembrane region of atl using the following primers:

Atl423 SacII F CAGCACGGACACCCGCGGTGTACTTC

Atl423 SacII R GAAGTACACCGCGGGTGTCCGTGCTG

The underline letters are the substituted nucleotides.

cDNA was mutated from wild-type atl-Myc/pcDNA3.1Zeo+ to have a tagged protein for biochemical and cell culture experiments. To introduce specific nucleotide substitutions in atlastin cDNA, site-directed mutagenesis was performed using Pfu Ultra HF DNA polymerase (Startagene). The basic procedure utilizes a supercoiled double-

stranded DNA (dsDNA) vector with an insert of interest and two synthetic oligonucleotide primers containing the desired mutation. The oligonucleotide primers, each complementary to opposite strands of the vector, are extended during temperature cycling by the Pfu Ultra DNA polymerase. Pfu Ultra DNA polymerase replicates both plasmid strands with high fidelity and without displacing the mutant oligonucleotide primers. Incorporation of the oligonucleotide primers generates a mutated plasmid containing staggered nicks. Following temperature cycling, the product is treated with DpnI. The DpnI endonuclease is used to digest the parental DNA template and to select for mutation-containing synthesized DNA.

PCR reaction

atl-Myc/pcDNA3.1Zeo+ template	50 ng
Forward (10 uM)	2 ul
Reverse (10 uM)	2 ul
10 mM dNTPs	1 ul
10X Pfu Ultra Buffer	10 ul
Pfu Ultra HF DNA polymerase	2.5 U/ ul
H2O	to 50 ul

PCR cycle

95°C 30 seconds

95°C 30 seconds
55°C 1 minute
68°C 6 minutes
} 15 cycles

The reaction was placed on ice for 2 minutes and 10 U of the DpnI restriction enzyme was added to the amplification. The reaction was incubated at 37°C for 1 hour to digest the parental, non mutated, dsDNA.

Transformation

Ligation mixture was used for transformation of chemically competent DH5alpha cells (Invitrogen). Transformed bacteria were plated on LB–ampicillin agar plates and

incubated overnight at 37°C. Twelve colonies were grown in LB medium with ampicillin. Plasmid DNA was successively purified by minipreparation protocol (Appendix A) and tested by restriction analysis using EcoRI and SacII to confirm the insertion of the mutation.

Purification and linearization of atl423 in pcDNA3.1Zeo+ vector

Plasmid DNA containing the SacII restriction site was purified according to NucleoBond Xtra Midi purification protocols (Macherey-Nagel). The final pellets were re-suspended in 50 ul of TE buffer. 500 ng of atl423-Myc/pcDNA3.1Zeo+ was linearized using 1 ul of SacII restriction enzyme, at 37°C for 1 hour. The bands corresponding to the atlastin fragment was cut from gel and purified using the Nucleospin Extract II Kit (Macherey-Nagel). Purified DNA products were eluted in 20 ul of elution buffer. The sticky-ends generated were dephosphorylated as follows:

atl423-Myc/pcDNA3.1Zeo+	20 ul
10X Buffer SAP	3 ul
SAP (Fermentas)	1 ul

The mixture was incubated at 37°C for 1 hour and the enzyme was inactivated at 65°C for 15 minutes.

Insertion of the linker sequence in position 423 of atlastin/pcDNA3.1Zeo+

The linker sequence is generated by annealing of double-stranded oligo which codified for a sequence of glycine-glyicine-serine repeated three times. In order to verify the insertion of the linker sequence in the atl cDNA, the oligo are generated to create a restriction site for BamHI (underlined in the sequence). The oligo, phosphorilared at 5', were syntesized by Bio-Fab Research s.r.l. laboratories:

GGS-f P-CGGTGGATCCGGTGGTTCCGGAGGTTCCGC

GGS-r CGGCCACCTAGGCCACCAAGGCCTCCAAGG-P

The annealing reaction to create the double-stranded oligo was the following:

100 uM GGS-f
100 uM GGS-r
100 uM pH 7.5-8 Tris HCl
50 mM NaCl
1 mM EDTA

The reaction was incubated at 90°C for 5 minutes. Two different concentrations vector:insert (1:10 and 1:100) were ligated with the linearized atl423-Myc/pcDNA3.1Zeo+:

atl423-Myc/pcDNA3.1Zeo+	100 ng
linker sequence	1:10 or 1:100
10x Buffer T4 Ligase	1ul
T4 DNA Ligase Biolabs	1ul
H2O	to 10 ul

The mixture was incubated at room temperature for 1 hour.

Transformation and sequencing of mutated atlastin cDNA

Ligation mixture was used for transformation of DH5alpha cells (Invitrogen). Two clones of each construct have been sequenced to verify the presence and the number of insertion of the linker sequence. The DNA clones were sequenced by Bio-Fab Research using the following primer:

M13 Rev CAGGAAACAGCTATGAC

The sequences were analized using SequencherTM 4.8 (Gene Codes Corporation). It has been identified two clones containing one and three repetition of the linker sequence, respectively.

Purification of atl(1xlinker)-Myc and atl(3xlinker)-Myc in pcDNA3.1Zeo+

Plasmid DNA was purified from an overnight culture according to NucleoBond Xtra Midi purification protocols (Macherey-Nagel).

2.1.3 Generation of atlastin(1xlinker) and atlastin(3xlinker) in pUAST plasmid

Atlastin(3xlinker) cDNAs were subcloned in the pUAST vector for P-element mediated transformation (Appendix C). pUAST plasmid and atl(3xlinker)-Myc/pcDNA3.1Zeo+ were digested with EcoRI and XhoI restriction enzymes.

2.1.4 Cloning of wild-type DP1 cDNA in pcDNA3.1Zeo+ plasmid

The DP1 full-length complementary DNA was previously obtained by RT-PCR performed on total *Drosophila* RNA. The cDNA was cloned in pcDNA3.1Zeo+ vector (Appendix C). Myc tagged versions of DP1 was cloned in the pcDNA3.1Zeo+ plasmid. To insert the Myc epitope in the N-terminus of DP1, cDNA was amplified using the following primers:

Myc-DP1 BamHI F

5'AGCTGGATCCATGGAACAAAAACTTATTTCTGAAGAAGATCTGGCCACTC
AGGTGAAGCAGTTC3'

DP1 XhoI R

5'AGCTCTCGAGCTAGTCATGCTTCAGCACTCC3'

pcDNA3.1Zeo+ plasmid and PCR fragments were digested with BamHI and XhoI restriction enzymes.

2.1.5 Cloning DP1 cDNA in pUAST

Myc tagged versions of mutated DP1 were cloned in the pUAST plasmid (Appendix C). To insert the Myc epitope in the N-terminus of DP1, cDNA was amplified using the following primers:

Myc-DP1 NotI F

5'AGCTGCGGCCGCATGGAACAAAAACTTATTTCTGAAGAAGATCTGGCCAC
TCAGGTGAAGCAGTTC3'

DP1 XhoI R

5'AGCTCTCGAGCTAGTCATGCTTCAGCACTCC3'

PCR fragment were digested with NotI and XhoI restriction enzymes and cloned into pUAST vector previously linearized.

2.1.6 Quantitative Real-Time PCR

Reverse transcription polymerase chain reaction (RT-PCR) is one of many variants of polymerase chain reaction (PCR). This technique is commonly used in molecular biology to detect RNA expression levels. Quantitative RT-PCR (qRT-PCR) is considered to be the most powerful, sensitive, and quantitative assay for the detection of RNA levels. The quantification of mRNA using RT-PCR was achieved performing a one-step reaction. In the one-step approach, the entire reaction from cDNA synthesis to PCR amplification occurs in a single tube. The one-step approach is thought to minimize experimental variation by containing all of the enzymatic reactions in a single environment.

In order to test several DP1 RNAi lines we used the SuperScript III Platinum One-Step Quantitative RT-PCR System (Invitrogen).

DP1 RNAi lines were crossed with tubulin-GAL4, at 28°C; DP1 RNAi;tubulin-Gal4 were selected and the total RNA were isolated using Trizol (Invitrogen).

We designed specific DP1 primers that anneal within the exon/exon boundary of the mRNA to allow differentiation between amplification of cDNA and potential contaminating genomic DNA:

DP1 For Real-time	GCGATGCTTCCAAGCCGTGGA
DP1 Rev Real-time	GGTAGATGGCGCACAGACCA

The reaction was prepared as follow:

Total RNA	1 ul
Forward	0,2 ul
Reverse	0,2 ul
ROX Reference Dye	0,1 ul
2x Reaction mix	5ul
SuperScript III	0,2 ul
H2O	to10 ul

We choose RP49 as reference gene to avoid competition between amplification of the reference gene and sample gene. The qRT-PCR was performed using standard protocols.

2.1.7 Cloning of wild-type Reticulon cDNA in pcDNA3.1Zeo+ plasmid

The Rtnl1-PB isoform was obtained from the *Drosophila* Genomic Resource Center (LD14068). This cDNA was subcloned in-frame with an N-terminal HA or Myc tag in the pcDNA3.1Zeo+ vectors using the following primers:

Myc-Rtnl1-PB EcoRI F

AGCTGAATTCATGGAACAAAAACTTATTTCTGAAGAAGATCTGTCCGCATTTGGTGAAACC

HA-Rtnl1-PB EcoRI F

5'AGCTGAATTCATGTACCCATACGATGTTCCTGACTATGCGGGCTCCGCATTTGGTGAAACC3'

Rtnl1-PB XhoI R

5'AGCTCTCGAGCTTTACTTGTCCTTCTCAGAC3'

The PCR fragments and the pcDNA3.1/Zeo+ plasmid were digested with EcoRI and XhoI restriction enzymes

2.1.8 Cloning Reticulon cDNA in pUAST

HA tagged versions of mutated Reticulon were cloned in the pUAST plasmid (Appendix C). To insert the HA epitope in the N-terminus of reticulon, cDNA was amplified using the following primers:

HA-Rtnl1-PB EcoRI F

5’AGCTGAATTCATGTACCCATACGATGTTCCTGACTATGCGGGCTCCGCATTTGGTGAAACC

Rtnl1-PB XhoI R

5'AGCTCTCGAGCTAGTCATGCTTCAGCACTCC3'

pUAST plasmid and PCR fragment were digested with the appropriate restriction enzymes.

2.2 *Drosophila* transformation

2.2.1 Microinjection

The atl(3xlinker)-Myc/pUAST, Myc-DP1/pUAST, HA-Rtnl1/pUAST were prepared and sent to BestGene Inc. for *Drosophila* embryo injection. w^{1118} strain was used for microinjection. w^{1118} flies have white eyes, allowing the detection of the transgene insertion in the offspring.

2.2.2 Characterization of transgenic lines

Hatching adults (F0) were separated by sex and crossed to w^{1118} flies. The F1 offspring was screened for transformant individuals where exogenous DNA was inserted in the fly genome. Transgenic flies selected for the red eye phenotype will be crossed with "balancer" lines that carry dominant phenotypic markers to generate a stable transgenic line and avoid transgene loss. F1 individuals may bear one transgene insertion on any of the chromosomes: X, II, III or IV. Transgenes inserted on the fourth chromosome are very rare as this chromosome is rather small and essentially heterochromatic. Each transgenic F1 fly is crossed with the second chromosome balancer stock Sm6a/TfT, carrying the dominant morphological marker *CyO* that produces curly
wings. Individuals of the F2 carrying the transgene and the *CyO* marker were crossed to generate a stable transgenic line.

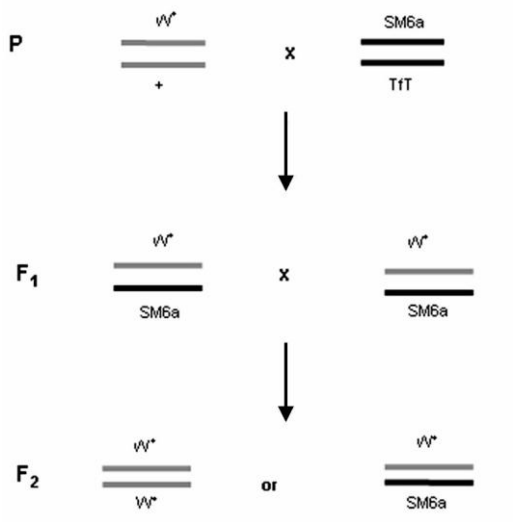

Fig. 4 Cross with II chromosome balancer

Each transgenic F1 fly is crossed with the third chromosome balancer stock TM3/TM6, carrying the dominant morphological marker *Sb* that produces stubble hairs. Individuals of the F2 carrying the transgene and the *Sb* marker were crossed to generate a stable transgenic line.

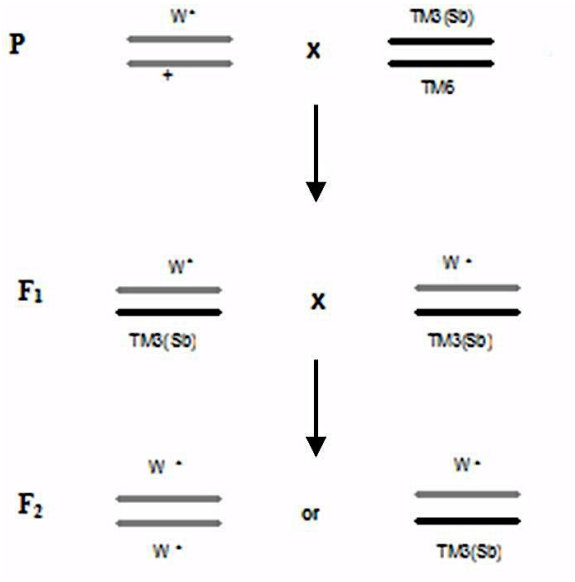

Fig. 5 Cross with III chromosome balancer

Each transgenic F1 male fly is crossed with the X chromosome balancer stock Fm7/Sno, carrying the dominant morphological marker *Bar* that produces heartshaped eyes. If the insertion is occurred in the X chromosome, all the F1 females have heart-shaped red eyes. These female were crossed with males of the X chromosome balancer stock Fm7/Y to generate a stable transgenic line.

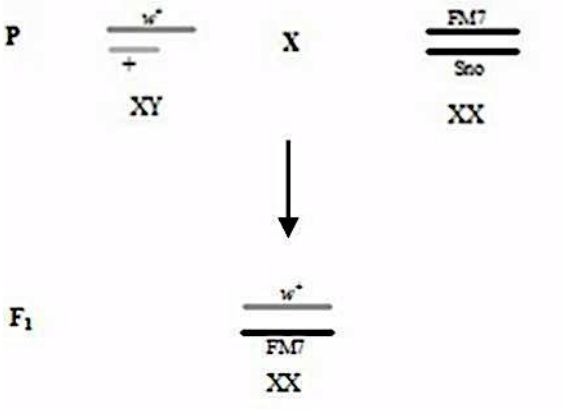

Fig. 6 Cross with X chromosome balancer

2.2.3 *Drosophila* genetics

Fly culture and transgenesis were performed using standard procedures.

Drosophila strains used: GMR-Gal4; tubulin-Gal4; tubulin-Gal4, KDEL-GFP.

Control genotypes varied depending on individual experiments, but always included promoter-Gal4/+ and UAS-transgene/+ individuals.

DP1-RNAi lines were obtained from Vienna *Drosophila* RNAi Center (KK-105290, GD-35377 and GD-35378).

Lifespan experiments were performed with 200 animals for each genotype. Flies were collected 1 day after eclosion and placed in vials containing 50 animals. The animals were maintained at 25°C, transferred to fresh medium everyday, and the number of dead flies was counted. Lifespan experiments were repeated at least 3 times.

2.2.4 Generation of DP1 knock-out flies

There are two general methods of gene targeting, called ends-in and ends-out. The ends-out method is a simple replacement of the genomic sequence with the homologous sequence. To carry out gene targeting in *Drosophila* a donor construct carrying DNA from the gene to be targeted is randomly inserted into the genome by P-element-mediated transformation. Then, a site-specific recombinase (FLP) and a site-specific endonuclease (*I-SceI*) are used to generate, *in vivo*, an extrachromosomal DNA molecule that carries a double-strand break (DSB) within the gene of interest. The presence of this DSB stimulates homologous recombination between the excised donor and the homologous chromosomal target locus (Rong and Golic, 2001). A typical strategy for knocking out a gene might be to interrupt that gene with a heterologous sequence, such as the mini-white marker.

The DP1 targeting construct was generated by cloning PCR-amplified 3 kb genomic fragments upstream and downstream of the DP1 open reading frame (ORF) using the following primers:

DP1 5’ KO F CACTGAAGGTGTCTGCTTCCGCGAA

DP1 5’ KO R GCATCTGGAAAGTCGGCGGCGTC

DP1 3’ KO F GGCGAATGTACCGTAGCTCCGACCG

DP1 3' KO R CGTCGTCTATCATCTGTTGCCGCAC

The resulting fragments were cloned into the pEndsout2 vector (Appendix C) upstream and downstream the mini-white gene. This construct was prepared for *Drosophila* embryo injection (see Microinjection 2.2.1) and F1 were balanced. The lines obtained were called donor lines.

Targeting crosses for DP1 gene disruption

To induce targeting, donor construct lines are crossed to the *P*{*hsp70::FLP*} *P*{*hsp70::I-SceI*} stock (Bloomington). The progeny are subjected to heat shock to induce FLP and *I-SceI*. We have heat-shocked on days 3 into a water bath at 38°C, for 90 minutes. Virgin females with the donor and the FLP and *I-SceI* constructs are collected when they eclose. These females should have white eyes, possibly with a few colored cells remaining, indicating FLP activity. These are crossed to males that constitutively express FLP, *P*{*70FLP*}*10* (Bloomington), and the progeny are screened for any with solid eye color. Each individual with homogeneous red eyes is crossed with different chromosome balancers to generate a stable transgenic line. All the potential DP1 knock out lines obtained will be tested by PCR and RT-PCR for confirming DP1 gene disruption.

2.3 Cell biology

2.3.1 HeLa and COS-7 cell culture

HeLa cell culture was derived from a cervical carcinoma of a 31 years old African-American woman. This was the first aneuploid line derived from human tissue maintained in continuous cell culture.

COS is a fibroblast-like cell line derived from monkey kidney tissue. COS cells are obtained by immortalizing CV-1 cells with a version of the SV40 virus that can produce large T antigen but has a defect in genomic replication. The CV-1 cell line in turn was derived from the kidney of the African green monkey. Two forms of COS cell lines commonly used are COS-1 and COS-7.

2.3.2 Propagation, subculturing and transfection

We used standard protocols for propagation, subculturing and transfection of both HeLa and COS-7 cells. Cells were grown in complete DMEM medium (Lonza) with 10% FBS serum and antibiotics, at 37°C in a CO_2 incubator. Cells were passaged at 70 to 80 % confluency.

To introduce expression plasmids into cells *Trans*IT-LT1 Transfection Reagent (Mirus Bio) was used.

2.3.3 Immunocytochemistry (ICC)

For immunocytochemistry, the day before transfection cells were plated on a glass coverslip previously sterilized.

One day after transfection, the cells were fixed in 4% paraformaldehyde in PBS pH 7.4 for 10 minutes at room temperature. The cells were then washed tree times with PBS to eliminate paraformaldehyde.

To permeabilize cell membranes and improving the penetration of the antibody, the cells were incubated for 10 minutes with PBS containing 0.1% Triton X-100 (Applichem). Cells were incubated with 10% serum in PBS for 10 minutes to block non specific binding of the antibodies. Primary antibodies, diluted in PBS with 5% serum, were applied for 1 hour in a humidified chamber at 37°C. Cells were washed three times with PBS and then secondary antibodies, diluted in PBS, were applied for 1 hour in a humidified chamber at 37°C.

Coverslips were mounted with a drop of the mounting medium Mowiol.

The following antibodies were used: mouse anti-Myc (1:1,000, Sigma), and rabbit anti-HA (1:500, Santa Cruz Biotechnology), mouse anti-PDI (1:200, BD Biosciences), rabbit anti-calnexin, GFP-Sec61β (provided by Gia Voeltz), anti-GM130 (1:200, BD Biosciences). Secondary antibodies for immunofluorescence (Cy5 and Cy3 conjugates from Jackson Laboratories and Alexa Fluor 488 conjugates from Invitrogen) were used at 1:1000.

2.4 Microscopy

2.4.1 Electron microscopy (EM)

Drosophila brains were fixed in 4% paraformaldehyde and 2% glutaraldehyde and embedded. EM images were acquired from thin sections under a FEI Tecnai-12 electron microscope. EM images of individual neurons for the measurement of the length of ER profiles were collected from three brains for each genotype. At least 20 neurons were analyzed for each genotype. Quantitative analyses were performed with ImageJ software.

2.4.2 Image analysis

Confocal images were acquired through x40 or x60 CFI Plan Apochromat Nikon objectives with a Nikon C1 confocal microscope and analyzed using either Nikon EZ-C1cor NIH ImageJ softwares. Figure panels were assembled using Adobe Photoshop CS4.

In the quantification experiment, seven independent transfection experiments were performed and approximately 100 cells were scored in each experiment.

P values reported in this study are two tailed values and derived from a Student's t-test, assuming unequal variances. Standard errors are reported as S.E.M.

APPENDIX A: General protocols

Transformation of chemiocompetent cells

- Gently thaw the chemiocompetent cells on ice.
- Add ligation mixture to 50 ul of competent cells and mix gently.
- Incubate on ice for 30 minutes.
- Heat-shock the cells for 30 seconds at 42°C without shaking.
- Immediately transfer the tube to ice.
- Add 450 µl of room temperature SOC medium.
- Shake horizontally at 37°C for 1 hour.
- Spread 20 ul and 100 ul from the transformation on pre-warmed selective plates and incubate overnight at 37°C.

Preparation of plasmid DNA by alkaline lysis with SDS: minipreparation

- Inoculate 3 ml of LB medium (Appendix B) containing the appropriate antibiotic with a single colony of transformed bacteria. Incubate the culture overnight at 37°C with shaking.
- Pour 1.5 ml of the culture into a microfuge tube. Centrifuge at maximum speed for 30 seconds in a microfuge. Store the unused portion of the original culture at 4°C.
- Remove the supernatant.
- Resuspend the bacterial pellet in 100 ul of ice-cold Alkaline lysis solution I (Appendix B) by vortexing.
- Add 200 ul of Alkaline lysis solution II (Appendix B) to each bacterial suspension. Mix by inverting the tube five times.
- Add 150 ul of ice-cold Alkaline lysis solution III (Appendix B). Close the tube and disperse Alkaline lysis solution III through the viscous bacterial lysate by inverting the tube several times. Incubate the tube on ice for 3-5 minutes.
- Centrifuge the bacterial lysate at maximum speed for 10 minutes at 4°C in a microfuge. Transfer the supernatant to a fresh tube.

- Precipitate nucleic acids from the supernatant by adding 2 volumes of ethanol at room temperature. Mix the solution by vortexing and then allow the mixture to stand for 2 minutes at room temperature.
- Collect the precipitate of nucleic acid by centrifugation at maximum speed for 15 minutes at 4°C in a microfuge.
- Remove the supernatant.
- Add 2 volumes of 70% ethanol to the pellet and invert several times.
- Recover the DNA pellet by centrifugation at maximum speed for 5 minutes at 4°C in a microfuge.
- Remove carefully all the ethanol by gentle aspiration.
- When the pellet is dry, dissolve the nucleic acids in 50 ul of distilled water containing 20 ug/ml DNase-free RNase A. Vortex the solution gently for a few seconds. Store the DNA solution at -20°C.

APPENDIX B: Stocks and solutions

LB Medium (Luria-Bertani Medium)

Bacto-tryptone 10g

Yeast extract 5g

NaCl 10g

H2O to 1 Liter

Autoclave

LB Agar

Bacto-tryptone 10g

Yeast extract 5 g

NaCl 10 g

Agar 20g

H2O to 1 Liter

Adjust pH to 7.0 and autoclave

LB–Ampicillin Agar

Cool 1 Liter of autoclaved LB agar to 55° and then add 100 ug/ml filter-sterilized ampicillin. Pour into petri dishes (~25 ml/100 mm plate).

SOC medium

Bacto-tryptone 20g

Yeast extract 5 g

NaCl 0,5 g

KCl 1M 2,5 ml

H2O to 1 Liter

Adjust pH to 7.0, autoclave and add 20 ml of sterile 1 M glucose

Alkaline lysis solution I

Glucose 50 mM

Tris HCl 25 mM (pH 8.0)
EDTA 10 mM (pH 8.0)

Alkaline lysis solution II

NaOH 0.2 N
SDS 1%

Alkaline lysis solution III

Potassium acetate 3 M
Glacial acetic acid 11.5%

TE Buffer

Tris-HCl 10 mM (pH 7.5)
EDTA 1 mM

Phoshate Buffered Saline (PBS)

KH2PO4 15 g/L
NaCl 9 g/L
Na2HPO4 8 g/L

***Drosophila*'s food**

Agar 15 g
Yeast extract 46.3 g
Sucrose 46.3 g
H2O to 1 Liter
Autoclave and then add 2 g of Nipagine dissolved in 90% ethanol

APPENDIX C: Plasmids

pcDNA3.1Zeo+ (Invitrogen)

pcDNA3.1Zeo+ is an expression vector, derived from pcDNA3.1, designed for high-level stable and transient expression in a variety of mammalian cell lines. To this aim, it contains Cytomegalovirus (CMV) enhancer-promoter for high-level expression; large multiple cloning site; Bovine Growth Hormone (BGH) polyadenylation signal; transcription termination sequence for enhanced mRNA stability.

pUAST vector

pUAST is a P-element based vector for transgenesis in *Drosophila*. It contains five tandemly Gal4 binding sites followed by the hsp70 TATA box and transcriptional start, a polylinker containing unique restriction sites and the SV40 small T intron and polyadenylation site. It also contains the white gene that allows the screening for successful incorporation of the transgene into the *Drosophila* genome. These features are included between the P-element ends (P3' and P5').

pEndsout2 vector

pEndsout2 is a vector for ends-out gene replacement in *Drosophila*. A genomic region is cloned into the polylinker, and the gene of interest is disrupted or replaced with the hsp70::white cDNA, which also serves as a marker for transformation. Externally to the polylinker, it has FRT sites adjacent to the *I*-sites.

3 RESULTS

3.1 Mechanism of atlastin mediated fusion

It has been previously demonstrated that atlastin requires its GTPase activity for membrane fusion *in vitro* (Orso *et al.*, 2009); however, the function of the other domains remains to be explored. We extended this work by conducting a systematic analysis of the domains of *Drosophila* atlastin important for its fusogenic activity.

3.1.1 Atlastin C-terminal cytoplasmic tail is required for membrane fusion

We started our studies by examining the mechanistic basis of nucleotide-dependent membrane fusion by atlastin using a structure-function analysis.

Drosophila atlastin (atl) is a 61-kDa multidomain protein (Fig. 7). It has a short N-terminal variable domain, followed by a well-conserved GTPase domain, a three-helix bundle (3HB) middle domain, two tandem transmembrane domains, and a C-terminal cytoplasmic domain.

We began our analysis by determining the region of atlastin required for membrane fusion by producing C-terminal truncations. We reasoned that significant N-terminal deletions would abolish fusion by impairing GTPase activity given that atl contains only a 14-residue N-terminal extension beyond the boundary of the GTPase domain. We thus generated two different constructs that removed the entire C-terminal cytoplasmic domain (residues 472–542) and a truncation that eliminated the second transmembrane domain as well as the C-terminal cytoplasmic domain (residues 451–542); both atl(1–471) and atl(1-497) retain an intact GTPase domain and at least one transmembrane anchor (Fig. 7). We produced atlastin truncation tagged at the 3' terminus in order to identify its localization when expressed in cell culture with specific anti-tag antibodies.

Because of atlastin role in homotypic fusion of endoplasmic reticulum membranes, we analyzed the consequences of the expression of truncated variants on ER morphology and compared them with the phenotypes induced by the expression of wild-type *Drosophila* atlastin.

When functional atlastin is overexpressed in mammalian cells, it correctly sorts to the ER, causes the formation of an enlarged ER compartment, and redistributes Golgi-resident proteins to the ER (Orso *et al.*, 2009). Figure 8 (A-C) shows the result of expressing wild-type atlastin in COS-7 cells. Atlastin co-localizes with the ER marker

Sec61β and produces significant changes in ER morphology. When we expressed atl(1–471), this truncated protein had an ER localization but minimally disrupted the ER morphology. This result demonstrates that atlastin lacking the entire C-terminal domain is a less- or non-functional protein *in vivo* (Fig. 8D-F).

We have demonstrated that the C-terminal cytoplasmic domain of atlastin is critical for membrane fusion. However, this region of atlastin is among the most divergent between atlastin homologs and paralogs. We further investigated the sequence of the C-terminal region using bioinformatics software. The region comprising the 470-541 aminoacids of 30 atlastins, including *Drosophila* atlastin, was aligned with ClustalW2 software. This closer inspection of the sequences revealed a ~25 aminoacids stretch of more highly conserved residues membrane-proximal to the second transmembrane domain followed by a very divergent extreme C terminus. So we subdivided the C-terminal cytoplasmic domain to add back the more conserved juxtamembrane region (residues 471–497). The resulting construct, atl(1–497), was also expressed in COS-7 cells and the ER morphology was examined. Figure 8 (G-I) shows that the overexpression of atl(1–497) results in a phenotype similar to that caused by overexpression of wild-type atlastin, confirming that atl(1–497) is functional *in vivo*.

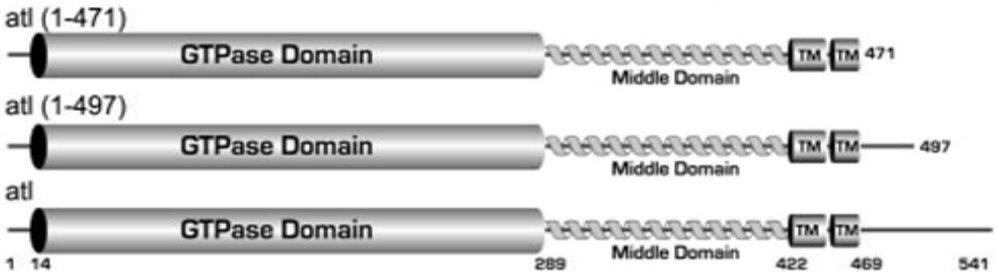

Fig. 7 The atlastin C-terminal cytoplasmic tail is required for membrane fusion
Domain structure of atl and C-terminal truncations. The GTPase domain is represented as a cylinder, the middle domain 3HB is shown as a helix, and the transmembrane domains are cylinders labeled "TM." Relevant domain boundaries are indicated by residue numbers above the diagram.

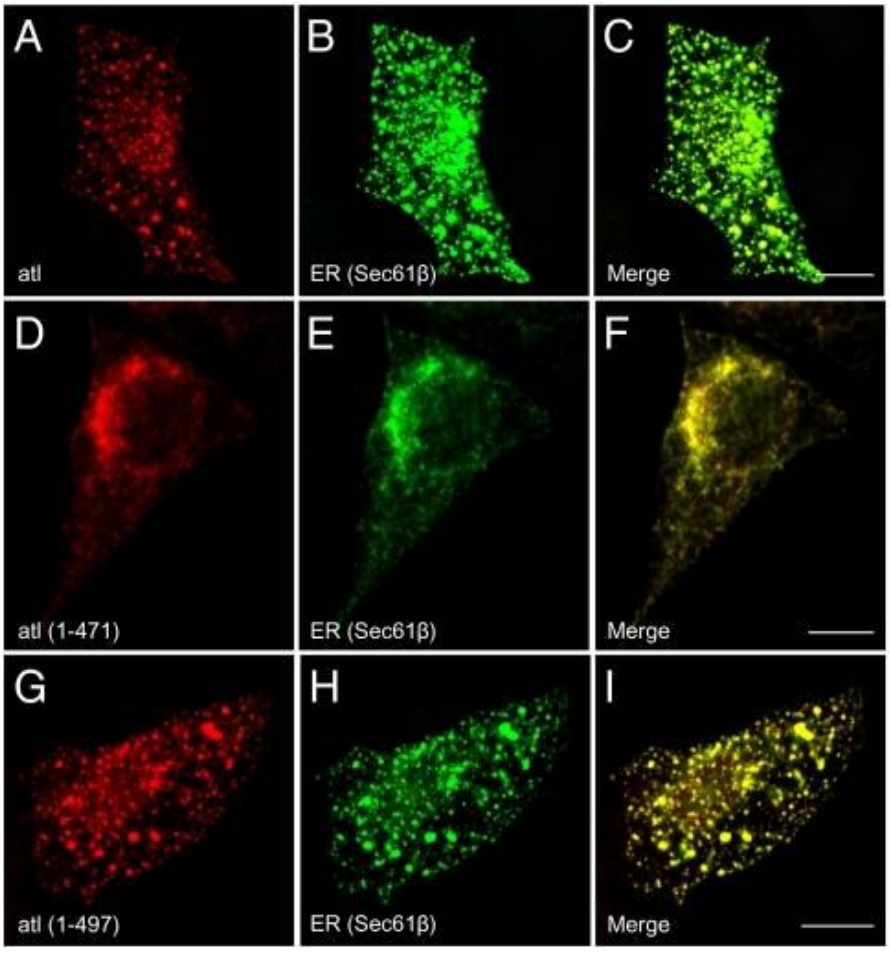

Fig. 8 Deletion of the atlastin C-terminal cytoplasmic tail results in a non-functional protein *in vivo*
COS-7 cells were cotransfected with wild-type atl-Myc (A–C), atl(1–471)-Myc (D–F), or atl(1–497)-Myc (G–I) and GFP-Sec61β. Wild-type atlastin and atl(1–497) show an abnormal, punctate ER, indicating a functional atlastin protein, whereas atl(1–471) localizes to a normally reticular ER, suggesting that it is a nonfunctional protein. Scale bar: 10 um.

3.1.2 The soluble N-terminal cytoplasmic domain of atlastin is a concentration-dependent inhibitor of ER membrane fusion

All membrane fusion proteins characterized to date require membrane integration. However, liberated soluble domains that retain the ability to productively interact with membrane integral components are often inhibitors of fusion. This is definitely the case for SNARE proteins, and inclusion of a soluble fragment of either v-SNARE or t-SNARE component will inhibit fusion (Weber *et al.*, 1998).

We tested the functionality of *Drosophila* atlastin C-terminal truncations that lack a membrane-spanning domain by determining their capacity to inhibit fusion. A construct containing the N-terminal GTPase domain and the 3-helix bundle was cloned in frame with the Myc tag sequence in a vector for expression in mammalian cell culture (Fig.9). The ability of the isolated N-terminal cytoplasmic domain to inhibit fusion was explored by co-overexpressing atl(1–422) in COS-7 cells with wild-type atlastin. We designed the experiment co-transfecting cells with increasing molar ratio of atlastin(1-541): atlastin(1-422) to find the best condition for analysis and quantification of the ER phenotype. Thus we set the protocol using atlastin(1-541):atlastin(1-422) in ratio 1:2.

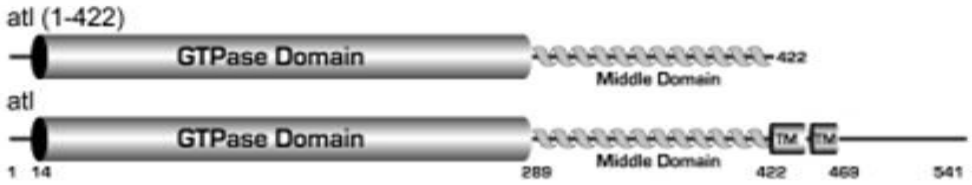

Fig. 9 Domain structure of atl
The middle domain is required for the inhibition of fusion by the N-terminal cytoplasmatic domain of atl.

As shown in Fig. 8 (A-C), overexpression of *Drosophila* atlastin in COS-7 cells disrupts ER morphology, presumably because of inappropriate and excessive ER fusion. However, simultaneous overexpression of the soluble N-terminal cytoplasmic domain of atlastin, atl(1–422), reduces the severity or largely prevents the aberrant ER structures generated by atlastin (Fig. 10). Cells co-transfected with wild-type and atl(1-422) were scored for endoplasmic reticulum morphology. A spectrum of inhibition is seen with atl(1–422), which likely reflects the relative degree of overexpression. When cells were subjectively binned into three groups, defined as normal ER morphology (Fig. 10A and D, empty arrowheads), fused ER (Fig. 10D and G, white arrowheads), and partially fused ER (Fig. 10G, gray arrowhead), more than half (56%) of the cells

expressing atl(1–422) exhibited a normal ER morphology, whereas 43% displayed a partially fused ER (Fig. 11). As a control, we co-transfected wild-type atlastin with a cytosolic GFP to determine whether the ER phenotype shown in the previous experiments was not due to the experimental procedure. If the control GFP is unable to inhibit the fusion reaction, atlastin will cause ER hyperfusion. In fact the totality of the cells co-transfected with atlastin and GFP showed a hyperfused ER morphology, indicating that atlastin fully retains its ability to fuse membranes (Fig. 11).

We interpret these results to suggest that atl(1–422) productively and preferentially interacts with full-length wild-type atlastin to inhibit its fusion activity *in vivo*.

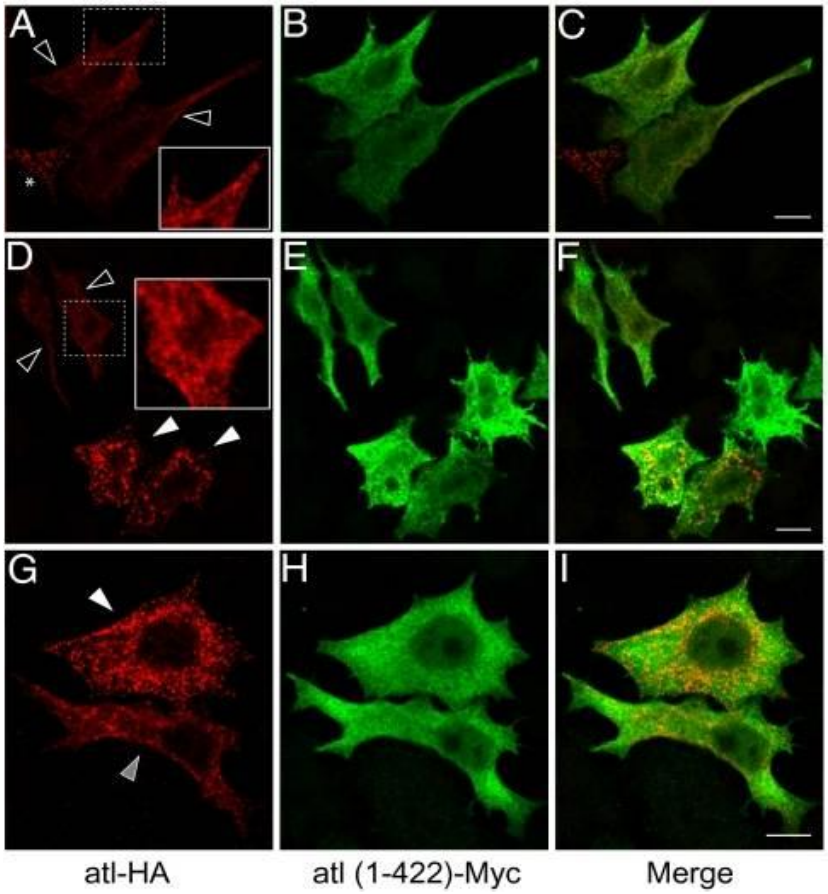

Fig. 10 Variable overexpression of the atlastin N-terminal cytoplasmic domain dominantly inhibits wild-type atlastin function *in vivo*

(A–C) COS-7 cells expressing both full-length atl and atl(1–422) show a relatively normal ER phenotype (empty arrowheads). Asterisk indicates a cell expressing full-length atl only and shows an abnormal, punctate ER phenotype. (D–F) COS-7 cells expressing full-length atl and varying levels of atl(1–422) show a mix of a normal ER phenotype (empty arrowheads) and a fused ER phenotype (white arrowheads). (G–I) COS-7 cells coexpressing atl and atl(1–422) representing a fused ER phenotype (white arrowhead) and a partially fused ER (gray arrowhead). Insets in A and D give a magnified view and increased color contrast of the outlined region of a cell showing the normal ER phenotype. Empty arrowheads indicate wild-type ER, where wild-type atlastin is inhibited by coexpression of atl(1–422). Gray arrowheads show the partially fused ER phenotype, where wild-type atlastin activity is partially inhibited by atl(1–422). White arrowheads illustrate fully fused ER, where there is minimal or no effect of atl(1–422). Scale bar: 10 um.

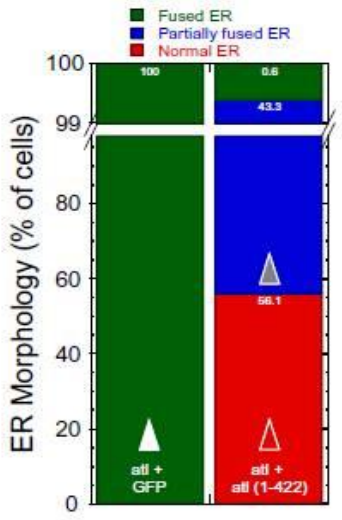

Fig. 11 Quantitation of atl(1–422) inhibition *in vivo*
The data shown in Fig. 10 are quantified as fused ER (green; white-filled triangle), partially fused ER (blue; gray-filled triangle), or normal ER (red; empty triangle). Note that 100% of the cells present a fused ER morphology when expressing only wild-type atlastin.

3.2 Distance of atlastin complex formation from the membrane is critical for fusogenic activity

The identification of SNARE proteins as basic components of the cellular fusion machinery (Weber *et al.*, 1998; McNew *et al.*, 1999) has permitted a detailed analysis of molecular parameters governing protein-mediated membrane fusion. Most SNARE proteins possess a single transmembrane domain at their extreme carboxy terminus and are predicted to have a high propensity to form coiled-coil structures. Assembled cytosolic domains of SNARE proteins form very stable structures in all cases that have been closely examined, likely due to their coiled-coil nature.

The 3HB middle domain of *Drosophila* atlastin is positioned four to five amino acid residues N-terminally to the transmembrane anchor. A consequence of this structural organization is that formation of trans-oligomers between atlastin 3HBs would bring apposed membranes into very close proximity to allow the atlastin complex to force membrane fusion. We thus examined the effects of progressively increasing the length of the juxtamembrane region of atlastin for fusion trough the insertion of a linker. We introduced a flexible linker containing the sequence (GGS)x3, repeated one or three times, between the 3-helix bundle and the first transmembrane domain of *Drosophila* atlastin (Fig. 13A). The linker sequence is composed of the three aminoacid repeat sequence glycine-glycine-serine repeated three times, (GGS)3x. These aminoacids were chosen because glycine has no side chain to restrict rotational freedom and likely adopts a random coil. This modification served two important functions: first, it relieved potential strain by introducing flexibility, and second, it extends the SNARE core helix

from its trans-membrane domain and presumably distances SNARE complex formation from the lipid bilayer interface.

The cDNA of atlastin, cloned in the vector pcDNA3.1Zeo+ for expression in mammalian cells, was mutagenized at position 1269 generating a SacI restriction site for the introduction of the linker sequence. The SacI site has been generated in such a way that the normal reading frame of *Drosophila* atlastin is maintained. The double-strand oligonucleotide coding for the linker was created to generate sticky-ends complementary to those produced by the artificial SacI site introduced in the atlastin sequence. After SacI linerization of the atlastin cDNA, the linker sequence was ligated. We prepared two ligation mixtures with different concentration of double-strand oligonucleotide favoring the insertion of more than one linker repetition. Finally, the linker oligonucleotide was designed to contain a restriction site recognized by BamHI; the digestion of the atlastin cDNA with this unique endonuclease site confirmed the appropriate insertion of the linker sequence. The positive clones were sequenced to evaluate the number of linker sequences inserted. We thus generated constructs for the expression in mammalian cells of atlastin containing one or three tandem copies of the linker, atl(1xlinker) and atl(3xlinker). Figure 13A shows the results of the linker mutations.

Our hypothesis was that the presence of the linker sequence moves complex formation farther away from the lipid bilayer interface. In this situation the tethering of opposing membranes could be more difficult compared to a physiological condition resulting in the inhibition of membrane fusion.

If the distance between the 3-helix bundle and the transmembrane domain of atlastin is important for the protein fusogenic activity, the insertion of a linker could inactivate atlastin-mediated fusion.

To verify our hypothesis, we expressed atlastin(1xlinker) and atlastin(3xlinker) in HeLa cells, analyzed the subcellular localization and the consequences of the expression of atlastin(linker) proteins on ER morphology and compared with the phenotypes induced by the expression of wild-type atlastin. In contrast to controls, transfected HeLa cells overexpressing *Drosophila* atlastin displayed ER spots, likely owing to enlargement caused by excessive membrane fusion, and a dispersed Golgi apparatus (Fig. 12), indicating that spotty ER and redistribution of Golgi markers can be used as a read-out for atlastin function in mammalian cells.

Transfection of both atlastin(1xlinker) and atlastin(3xlinker) constructs did not cause alteration of ER localization or ER and Golgi morphology (Fig. 13B and Fig. 14). This result suggests that linker-containing atlastin sorted accurately but had lost its fusogenic properties.

This result was further confirmed by *in vivo* experiments in *Drosophila*. We found that unlike expression of wild-type atlastin which is lethal when expressed ubiquitously *in vivo*, expression of transgenic atlastin(3xlinker) in flies permitted normal adult viability. Moreover, overexpression of atlastin using the eye specific driver GMR-Gal4 gave rise to a small and rough eye phenotype (Orso *et al.*, 2009), which was completely suppressed by co-expression of atlastin(3xlinker) under the control of the same driver (Fig. 15A-B). These results provide evidence that the distance of atlastin complex formation from the membrane interface is an essential determinant of atlastin's fusogenic properties.

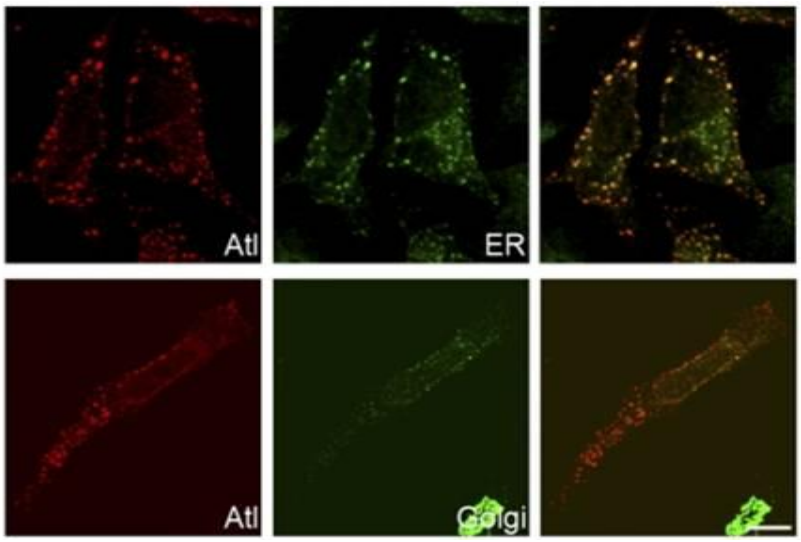

Fig. 12 Transfection of wild-type atlastin in HeLa cells results in the formation of enlarged ER and redistribution of Golgi proteins. Scale bar, 10 um.

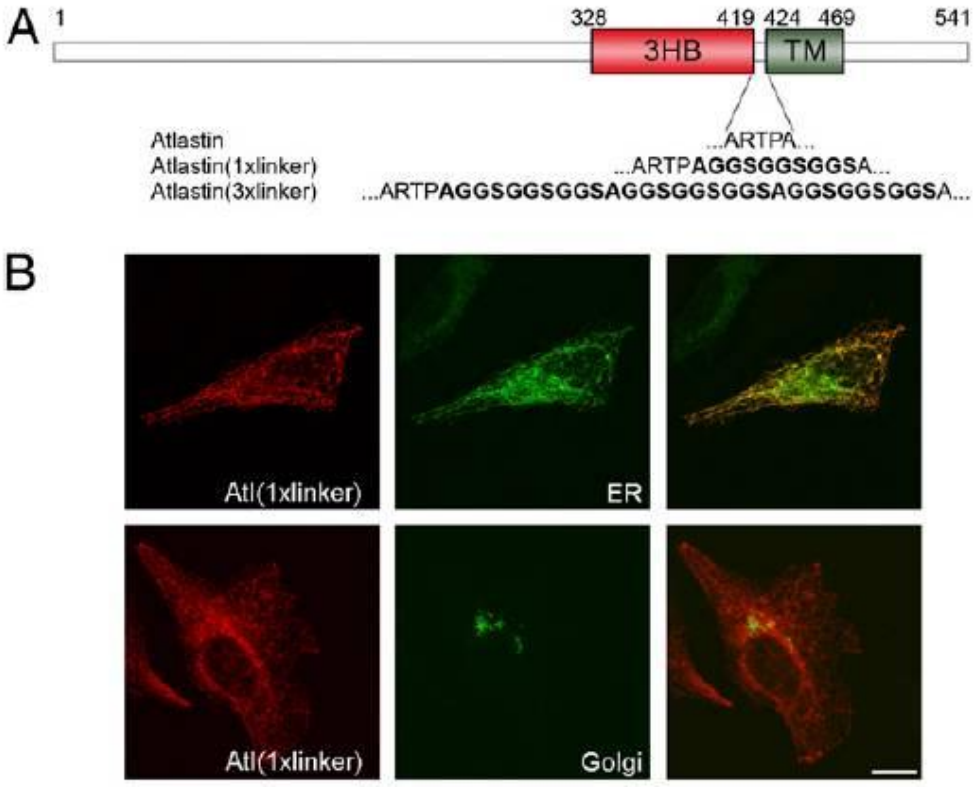

Fig. 13 Increasing the distance between the 3HB and the transmembrane domain causes inactivation of atlastin without inhibiting its oligomerization ability

(A) Sequence of full-length atlastin is represented, and the juxta-membrane region is magnified. The distance between the 3HB and the transmembrane domains was increased by introducing one or three copies of a linker containing the sequence (GGS)x3. (B) ER and Golgi morphology is unperturbed in HeLa cells transfected with atl(1xlinker). PDI and GM130 were used as ER and Golgi markers, respectively. Scale bar, 10 um.

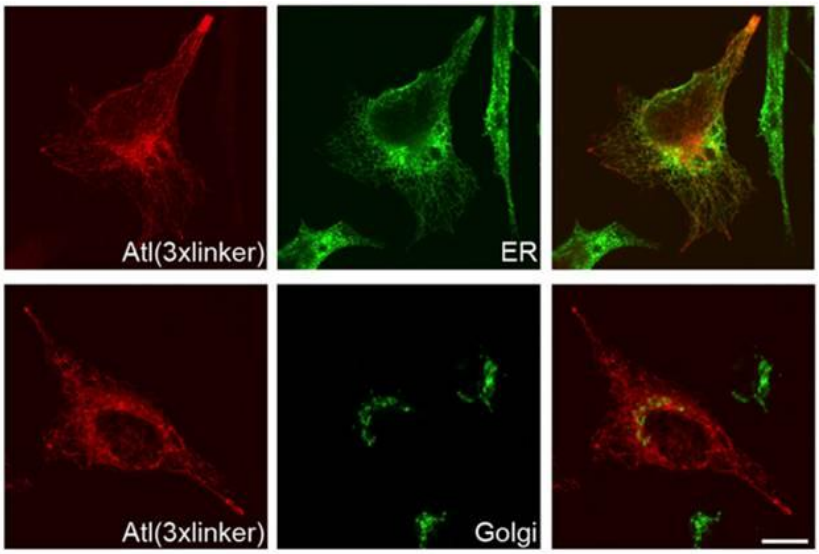

Fig. 14 Increasing the distance between the 3HB and the membrane anchor causes inactivation of atlastin

Endoplasmic reticulum (ER) and Golgi morphology is unperturbed in HeLa cells transfected with atlastin(3xlinker); PDI and GM130 were used as ER and Golgi markers, respectively. Scale bar, 10 um.

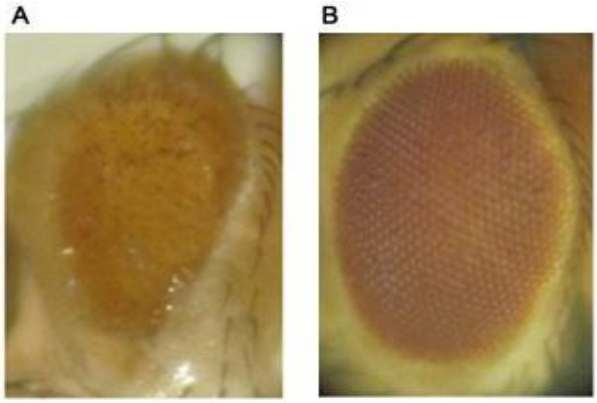

Fig. 15 (A) Overexpression of atlastin under the control of GMR-Gal4 causes a small eye phenotype. (B) GMR-Gal4 driven overexpression of atlastin(3xlinker) has no phenotypic consequences.

3.3 Atlastin functional partners

Human atlastins have been shown to interact physically with the ER tubule-shaping proteins reticulons and DP1. Moreover, in yeast a synergistic functional interaction has been proposed between the single atlastin homolog, the reticulon (Rtn1p and Rtn2p), and DP1 homologs (Yop1p).

Yeast cells lacking Rtn1p, Rtn2p, or both are viable, and, even in the double-deletion mutant, the morphology of the peripheral ER network appeared normal. Instead, *S. cerevisiae* lacking both reticulons and Yop1p had disrupted peripheral ER under normal growth conditions, while the nuclear envelope appeared to be unaffected. The triple-knockout mutant grew at about 2/3 the rate of wild-type cells. ER morphology defects similar to those in the triple mutant were also seen in mutants lacking Rtn1p and Yop1p. The ER appeared similar to wild-type in mutants lacking Rtn2p and Yop1p, although about 10% of the cells showed peripheral ER sheets. (Voeltz *et al.*, 2006).

In yeast lacking only the atlastin homolog Sey1p, the ER resembled that in wild-type cells, comparable to observations made previously for single deletions of Rtn1p or Yop1p (Voeltz *et al.*, 2006). In cells lacking both Sey1p and Rtn1p the cortical ER was severely perturbed; most cells lacked the tubular network and instead showed aberrant structures. Similar results were obtained with cells lacking Sey1p and Yop1p. Together, these results indicate that in yeast Sey1p cooperates with Rtn1p and Yop1p to maintain the structure of the tubular ER (Hu *et al.*, 2009).

3.3.1 Reticulon and atlastin display an antagonistic genetic interaction

To address the function of reticulon in the shaping of endoplasmic reticulum membranes in a multicellular organism *in vivo*, we investigated whether the single functional *Drosophila* reticulon gene, Rtnl1, interacts with the single ER membrane fusion protein atlastin in flies.

Null mutant lines for both reticulon and atlastin, called $Rtnl^1$ and atl^2, are available. Lee *et al.* have generated deletion mutants by imprecise excision of atl^1, a viable P-element insertion in the first intron of the *Drosophila* atlastin gene. Among the mutants, atl^2 had an approximately 1.6 kb deletion within the atlastin locus that removed the DNA encoding exon 3 through exon 4. The atlastin gene is essential, since mutants bearing the atl^2 allele as a homozygote survive only to pupal stages with few adult escapers. The escapers have smaller body sizes compared to w^{1118} wild-type control flies and are sterile (Lee *et al.*, 2009).

It is also available a *Drosophila* Rtnl1 loss-of-function line. Flies homozygous for the Rtnl1 mutation (referred to as $Rtnl1^1$) are viable, fertile and exhibit no obvious developmental abnormalities. To determine whether $Rtnl^1$ flies nevertheless exhibit subtle defects, the $Rtnl^1$ mutation was backcrossed into an isogenised background and compared the lifespan of these flies to their isogenic w^{1118} controls. Strikingly, $Rtnl1^1$ flies maintained at 29°C show a significant decrease in median lifespan. A similar reduction in median lifespan was also observed for $Rtnl1^1$ flies maintained at room temperature (Wakefield and Tear, 2006).

In order to investigate the presence of a potential genetic interaction between atlastin and reticulon, we performed a series of genetic crosses to generate the double mutant strain atl^2;$Rtnl^1$ that lack simultaneously both genes. We first analyzed flies lacking atlastin or reticulon separately.

In agreement with Lee *et al.* and Wakefield and Tear, homozygous atl^2 individuals die at the pupa stage with a 2% rate of escapers (Fig. 16a), while homozygous $Rtnl^1$ flies are viable and normal. Surprisingly, we found that combining the two mutations in homozygosity resulted in 84% adult survival (Fig. 16a), demonstrating that loss of $Rtnl^1$ rescues the lethality associated with depletion of atlastin. Thus, a strong antagonistic genetic interaction between atlastin and reticulon exists in *Drosophila*. Although viable, the fertility and the body size of atl^2;$Rtnl^1$ flies are not rescued: in fact double mutant flies are sterile and have a small body size. Moreover, the lifespan of atl^2;$Rtnl^1$ is half

compared to double heterozygous mutants (Fig. 16b) indicating that animals lacking both genes predictably do not fare well.

To analyze how the modulation of $Rtnl^{1}$ dosage affects ER morphology, we used electron microscopy (EM) to visualize the neuronal ER in third instar larva brains (Fig. 17). Ultrastructural analysis showed that in control neurons ER profile length (862±58 nm) was consistent with that previously reported (Orso *et al.*, 2009), while $Rtnl^{1}$ neurons displayed very elongated ER profiles (1981±178 nm). Re-expression of transgenic reticulon in $Rtnl^{1}$ flies led to restoration of the wild-type phenotype (Fig. 17). Remarkably, in atl^{2};$Rtnl^{1}$ double mutant the rescue of viability was accompanied by a robust rescue of ER length. In fact, double mutant ER profiles had an average length (1081±99 nm) comparable to that of normal profiles. The longer ER profiles found in $Rtnl^{1}$ mutants and the suppression of atlastin-induced ER fragmentation suggest that *in vivo* Rtnl1 may oppose atlastin fusogenic activity by mediating the fission of ER membranes. Consistent with this, EM analysis showed that in motor neurons overexpressing Rtnl1 the average ER profile length was about half (542±28 nm) that of controls providing direct evidence that ectopically expressed Rtnl1 causes fragmentation.

We confirmed the interaction between atlastin and Rtnl1 in transfected cell lines (Fig. 18). We cloned in an expression vector the reticulon cDNA, HA tagged at the N-terminus. Using reticulon and atlastin differentially tagged have permitted to screen only co-transfected cell and verify the localization of both reticulon and atlastin. Co-trasfected COS-7 cells were also stained with the ER markers calnexin. We expected that cells expressing only atlastin had an ER hyperfused phenotype, instead, cells expressing both reticulon and atlastin could show a rescue of the ER morphology (Fig. 18b-c). In fact, COS-7 cells transfected with wild-type *Drosophila* atlastin exhibit a hyperfused ER (Fig. 18a). Confirming our hypothesis, we found that over 40% of the cells co-expressing atlastin and Rtnl1 show a morphologically normal, reticular ER (Fig. 18e) showing that Rtnl1 has the ability to contrast the function of atlastin. These data provide substantial evidence that atlastin and reticulon act antagonistically in higher eukaryotes.

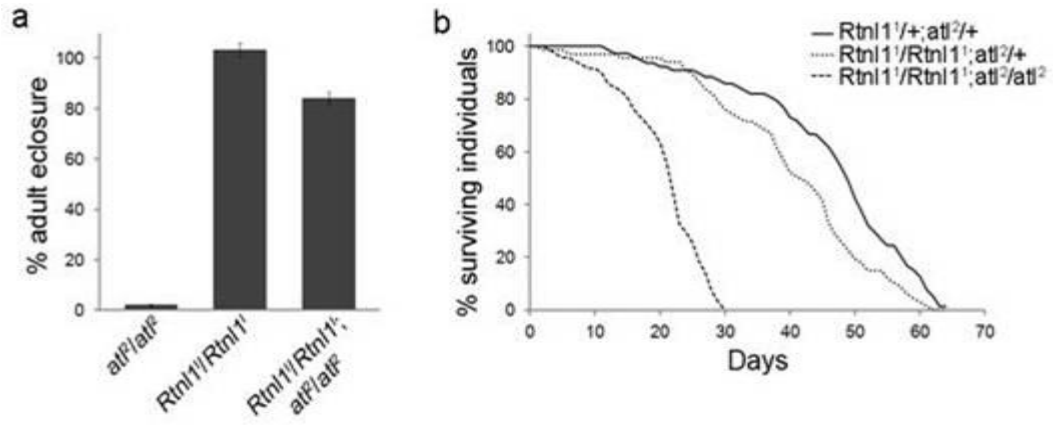

Fig. 16 Atlastin and Rtnl1 show opposing activities

(a) The histogram displays the percentage of surviving adults, expressed as the ratio of observed over expected individuals, for the indicated genotypes. (b) Longevity curve showing that *Rtnl1*^{1}/*Rtnl1*^{1};*atl*^{2}/*atl*^{2} double mutant flies have shortened lifespan.

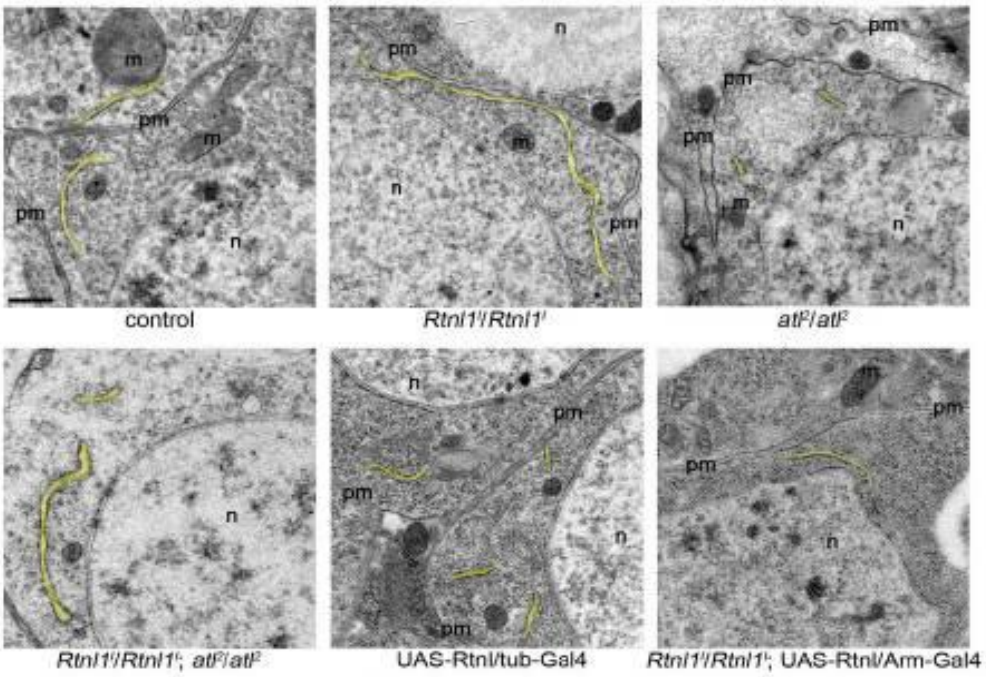

Fig. 17 Modulation of Rtnl1 levels affects ER morphology

Representative EM images of ventral ganglion neuronal bodies. ER profiles are highlighted. Scale bar 0.5 um. pm, plasma membrane; m, mitochondria; n, nucleus.

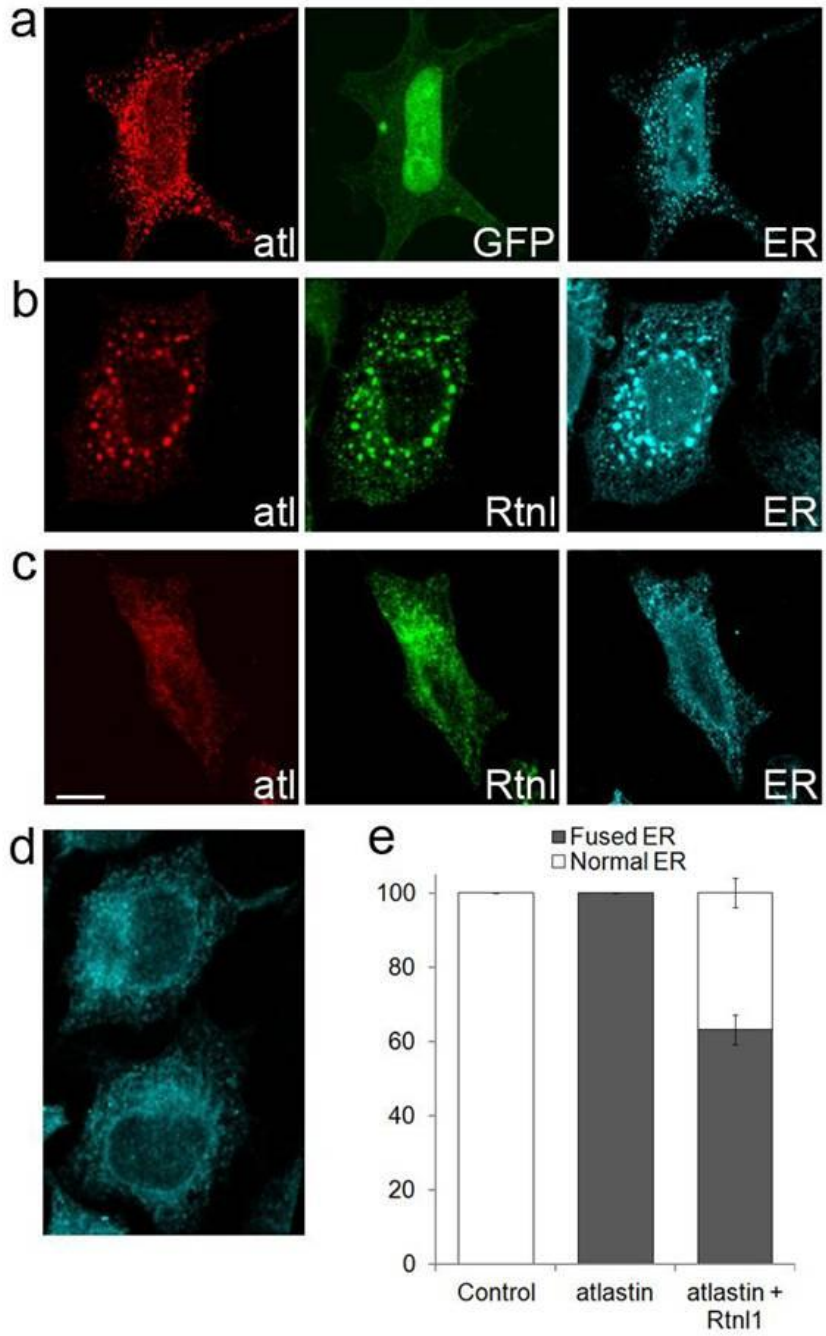

Fig. 18 Rtnl1 partially suppresses the atlastin-induced ER phenotype in COS-7 cells
(a) 100% of COS-7 cells transfected with wild-type atlastin-Myc and soluble GFP as co-transfection control show the typical atlastin-induced hyperfused ER. (b, c) In contrast, two phenotypic classes were observed upon co-transfection of wild-type atlastin-Myc and HA-Rtnl1. One class of cells displays the atlastin-induced abnormal ER morphology (b). In the other class the ER is normally reticular due to suppression of the atlastin phenotype by Rtnl1 (c). (d) Control untransfected cells show normal ER staining (e) Quantification of the relative abundance of the two phenotypic classes shown in (b, c). The ER is labeled with anti-calnexin. Scale bar, 10 um.

3.3.2 DP1 and atlastin interact genetically

Like reticulon, Deleted in Polyposis protein 1 or DP1 seems to be involved in the generation of tubular ER (see Introduction 4.3). The *Drosophila* genome contains only one highly conserved DP1 ortholog, CG8331, a situation that facilitates the study of this protein.

Null mutant *Drosophila* lines for DP1 are currently not available. We have tried to generated DP1 knock-out (KO) flies by gene targeting through ends-out homologous recombination. First, we generated the DP1 targeting construct consisting of a mini-white marker gene flanked by genomic sequences surrounding the DP1 open reading frame (ORF) (Fig. 19a). Specific primers were designed which amplified about 3 Kb genomic fragments up and downstream the DP1 ORF. The obtained fragments were cloned in the destination vector pEndsout2. This vector is specific for gene targeting because it contains the sequence encoding the mini-white marker gene and the sequence FLP and *I-SceI* that permits the homologous recombination between the DP1 gene and the targeting construct. In order to verify the presence and the correct order of the 3' and 5' fragments around the DP1 ORF and the mini-white PCR reaction were performed using specific primers as designed in figure 19A. PCR products at 3 Kb represent the amplification of mini-white and the amplification of the homology arms (primer pairs 1-2, 3-4 and 5-6) (Fig. 19b). The correct insertion of all the sequences in the pEndsout2 is verified using the primer pairs 1-7 and 8-6 thus obtaining PCR products at 5 Kb (Fig. 19b). After microinjection of the final plasmid in w^{1118} *Drosophila* embryos, two transgenic donor lines were obtained and balanced. To induce targeting, donor lines are crossed and heat shocked with flies ubiquitously expressing a flippase protein (FLP). From the F1 progeny, we selected virgin females with white eyes possibly with a few colored cells remaining, indicating FLP activity. These are crossed to males that constitutively express flippase, and the progeny were screened for any with solid eye color. So, potential targeting events will be recognized as progeny with homogeneous colored eyes. Thanks to the activity of the FLP protein in both crosses, transgenic lines carrying the targeting donor construct will be generated and homologous recombination between the donor DNA and the endogenous DP1 locus will create a null allele by replacing the DP1 ORF with the mini-white transgene. Until now, we have not been able to isolate such an event but this effort is still underway. Single potential DP1 KO lines will be screened by genomic PCR and confirmed by reverse transcription

polymerase chain reaction (RT–PCR) on total RNA (Rossetto *et al.*, 2011). In order to verify the insertion of the donor transgene into the DP1 locus by homologous recombination, we will isolate genomic DNA and test the presence of the transgene by PCR. PCR experiments will demonstrate that the DP1 locus is present in w^{1118} control DNA but is not amplified from DP1 KO DNA. In contrast, PCR products amplified using primer sets mapping to the inserted mini-white marker and outside of the homology arms will be found only in DP1 KO DNA.

As an alternative loss of function approach we used RNAi. RNAi DP1 flies are viable at the Vienna *Drosophila* RNAi Centre (GD-35377, GD-35378 and KK-105290). To validate KK-105290 and GD-35377 RNAi lines, we tested if, in contrast to control flies w^{1118}, the trascriptional level of DP1 is reduced using quantitative Real-Time PCR (qRT-PCR).

Based on the sequence of DP1, we designed primers between two exons; the presence of an intron between the exons allows the differentiation between amplification of cDNA and potential contaminating genomic DNA. The amplicon size was about 100bp. In order to maximize the effect of the RNAi on the transcriptional level of DP1, we crossed putative RNAi lines with the ubiquitous driver tubulin-Gal4, at 28°C, and verified the presence of obvious phenotypes on the progeny. The F1 generation flies are viable and have no phenotypic abnormalities. Therefore, potential RNAi-DP1;tubulin-Gal4 flies were selected to isolate mRNA and qRT-PCR was performed. The level of DP1 mRNA was then compared to a control mRNA of the housekeeping RP49 gene. We found that both the lines have a 90% reduction of DP1 mRNA level in contrast to DP1 mRNA in wild-type flies, demonstrating that these RNAi are functional.

To further investigate the presence of a potential genetic interaction between atlastin and DP1, we analyze first flies lacking only DP1. We crossed RNAi-DP1 flies under the control of several driver lines both ubiquitous and tissue-specific. Under all experimental conditions tested, the flies are viable, have normal lifespan and the integrity and morphology of the ER appear rather normal, as judged by the staining pattern of the ER marker GFP-KDEL.

A physical interaction between atlastin and DP1 has been proposed in yeast (Hu *et al.*, 2009). However, the functional significance of this interaction remains unclear. To investigate this aspect further we extend our analysis considering both atlastin and DP1. First, we generated a construct for the expression of DP1 in cell lines. As for reticulon, the expression of an antagonistic protein is expected to suppress the disrupted ER

morphology induced by atlastin. Indeed, over 40% of the cells co-expressing atlastin and DP1 exhibit a reticular ER (Fig. 20). This experiment preliminary reveal that also DP1 has the ability to counteract the fusogenic activity of atlastin.

We confirmed the interaction between atlastin and DP1 in the *Drosophila* fly eye (Fig. 21). To generate *Drosophila* transgenic lines, the DP1 cDNA was cloned in the pUAST vector, which is designed for incorporation into the *Drosophila* genome, in frame at the N-terminus with a Myc epitope. This construct was microinjected in *Drosophila* embryos and the obtained transgenic lines were then mapped to a specific chromosome and balanced. To study the effects of DP1 overexpression, we took advantage of the UAS-Gal4 system. In the DP1/pUAST construct, DP1 is under the control of UAS, the yeast transcriptional activator Gal4 binding sequence. In the absence of Gal4, the transgene is inactive. When flies carrying UAS-DP1 are crossed to flies that express Gal4 in a specific tissue or cell type, the transgenic protein is expressed only in these tissues or cells. While overexpression of wild-type *Drosophila* atlastin with a number of ubiquitous and tissue specific promoters led to lethality during early development, overexpression of UAS-Myc-DP1 with the same drivers allowed survival of the flies. Moreover, ectopic expression of atlastin in the developing eye gave rise to a small and rough eye phenotype (Fig. 21c and Orso *et al.*, 2009). In contrast, overexpression of DP1 in an eye simultaneously expressing atlastin resulted in the rescue of the atlastin-dependent phenotype (Fig. 21d). Together these experiments strongly suggest that in *Drosophila* atlastin and DP1 display a robust antagonistic functional interaction.

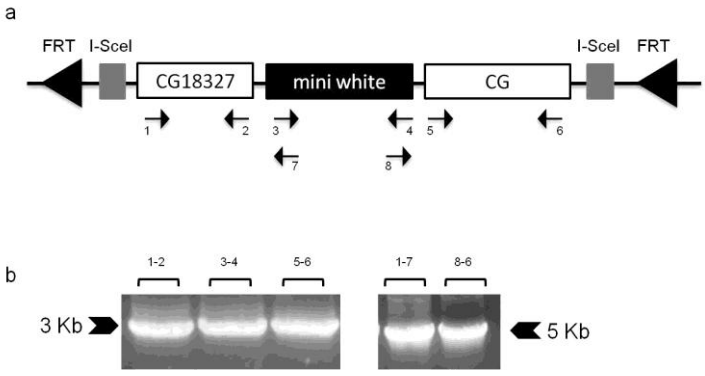

Fig. 19 Generation of donor transgene for DP1 KO

a) The targeting construct. These three sequences are inserted into the pEndsout2 plasmid. b) The presence of the three genomic sequences is tested by PCR.

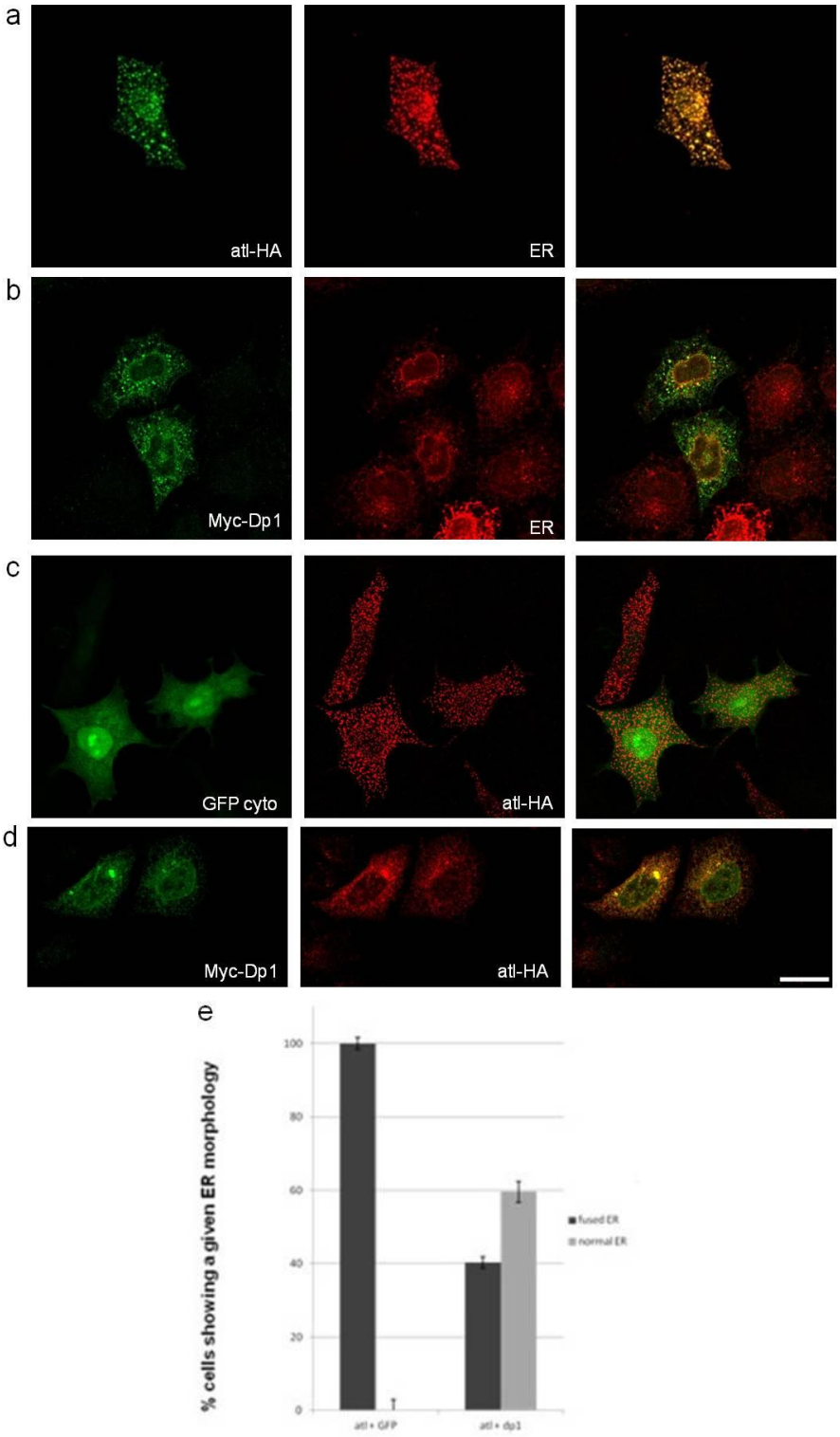

Fig. 20 Overexpression of DP1 rescues atlastin hyperfusion of ER membranes

(a) Overexpression in COS-7 cells of *Drosophila* atlastin-HA (green) induces hyperfusion of ER membranes, as shown by staining with calnexin (red). (b) COS-7 cells trasfected with Myc-DP1 (green) shows that it localizes to the ER (red) but does not perturb its morphology. (c) Hyperfusion of ER membranes caused by atlastin-HA (red) is not affected by cotrasfection of a "control protein" (GFP). (d) Cotrasfection in COS-7 cells of DP1 (green) and atlastin (red) leads to suppression of the atlastin-dependent hyperfusion phenotype. (e) Quantification of atlastin inhibition by coexpression of DP1. 100% of the cells coexpressing wild type atlastin and GFP display a hyperfused ER morphology. In contrast, 60% of cells cotransfected with atlastin-HA and Myc-DP1 show a normal ER morphology indicating suppression of atlastin fusogenic activity. Scale bar: 20 um.

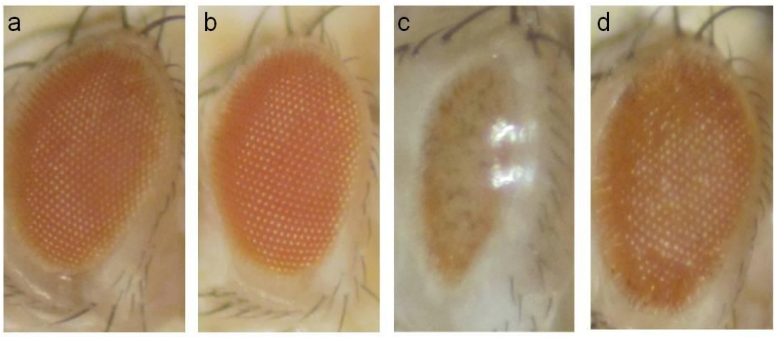

Fig.21 *Drosophila* atlastin and DP1 interact genetically

(a) Adult *Drosophila* eye (GMR-Gal4). (b) Eye overexpression of DP1 using GMR-Gal4 does not perturb the eye phenotype (GMR-Gal4/+; UAS-DP1/+). (c) Overexpression of atlastin using GMR-Gal4 generates a small eye (GMR-Gal4, UAS-atl/+). (d) The small eye produced by overexpression of atlastin is rescued by coexpression of DP1 under GMR-Gal4

4 DISCUSSION

The endoplasmic reticulum (ER) forms an elaborate network that spreads throughout the cell. Establishment and maintenance of proper architecture is essential for endoplasmic reticulum function. Homotypic membrane fusion is required for ER biogenesis and maintenance, and has been shown to depend on GTP hydrolysis. It has been demonstrated that *Drosophila* Atlastin, the fly homologue of the mammalian GTPase atlastin-1, involved in Hereditary Spastic Paraplegia, mediates membrane tethering and fusion of ER membranes. *Drosophila* atlastin forms transoligomeric complexes between adjacent ER membranes and promotes liposome fusion *in vitro*, and its over expression induces ER fusion *in vivo*, indicating that this GTPase is responsible for mediating ER homotypic fusion (Orso *et al.*, 2009).

The atlastins constitute a family of very closely related, integral membrane GTPases. They are distant members of the dynamin family of GTPases and are localized on the ER membrane. The *Drosophila* genome produces a single atlastin protein. *Drosophila* atlastin (atl) is 541 aminoacids long and has a predicted molecular mass of 61 kDa. The atl sequence is highly homologous to all three human isoforms, ranging between 44% and 49% identical over the entire length of the protein.

Despite the identification of the dual tethering and fusion-promoting role of *Drosophila* atlastin, it is not known how atlastin mechanistically brings about membrane fusion. The specific role(s) of GTP binding and/or hydrolysis during atlastin-mediated ER membrane fusion have not been determined.

Traditional membrane fusion proteins such as viral fusion proteins and SNAREs use energy derived from metastable protein folding intermediates to drive fusion. The use of chemical energy in the form of nucleotide hydrolysis at the point of membrane fusion is unique to atlastin, and perhaps mitofusins, and defines this class of membrane fusion proteins. Detailed analysis of this type of mechanism has only recently begun to be explored.

We have determined that a short region of about 27 amino acids located within the cytoplasmic C-terminal tail is critically required for atlastin-dependent membrane fusion *in vivo* and *in vitro*. In cellular system the insertion at the C-terminal of 27 aminoacids restore the functional ability of atlastin to fuse endoplasmic reticulum membranes. Moreover, no fusion was observed after reconstitution of these proteins into synthetic liposome. The functionality of these enzymes was confirmed by

examining GTPase activity. Atl(1–471) was able to cleave GTP at rates that were within about 30% of wild type rates, yet they were incapable of driving membrane fusion. The small reduction in GTPase activity for the C-terminal deletion mutants may reflect a subtle effect of the C-terminal tail on atlastin oligomerization.

Although we know that atlastin GTPase activity is required for membrane fusion, we know very little regarding the enzymatic properties of atlastin. We tested the functionality of C-terminal truncations that lack a membrane-spanning domain by determining their capacity to inhibit fusion between proteoliposomes that contain wild type atlastin. The N-terminal cytoplasmic domain (residues 1–422), when freed from membrane attachment, functions as a fusion inhibitor. *In vitro* experiments were performed in collaboration with the laboratory of James McNew at Rice University (Houston). When atl(1–422) was titrated into a fusion reaction containing wild type atlastin in the membrane, progressive inhibition of both the rate and extent of membrane fusion was seen. Inhibition was concentration-dependent, and fusion was completely inhibited with an eightfold molar excess of the atl(1–422) soluble domain. Although the full-length N-terminal cytoplasmic domain was a potent inhibitor, neither the isolated GTPase domain nor the soluble C-terminal tail inhibited fusion. Furthermore, quantitative analysis of the enzymatic properties of atlastin revealed that the N-terminal cytoplasmic domain is a more active enzyme than the full-length protein in detergent solution. However, reconstitution of the full-length protein into a phospholipid bilayer improved activity but not to the level of the soluble protein

An essential determinant of atlastin fusogenic ability is the distance of complex formation from the membrane. Increasing this distance results in the uncoupling of atlastin tethering and fusogenic abilities. Indeed, atlastin containing a 9-aa linker inserted between the α9 helix and the membrane anchor was incapable to fuse membranes either in HeLa cells or *in vitro*. Atlastin(1xlinker) was essentially unable to support liposome fusion *in vitro*, despite its normal GTPase activity, confirming that this mutant specifically lacks fusogenicity. To determine whether loss of fusogenicity may be due to the inability to oligomerize, coimmunoprecipitation assays were also performed. These experiments demonstrated that complex formation ability was retained by atlastin with linker even in the most severe case (3xlinker), suggesting that linker insertion does not prevent correct protein folding. Thus, a small increase in the separation between the 3HB and trans-membrane domains induces protein inactivation without inhibiting atlastin oligomerization properties. Insertion of a similar linker

between the transmembrane domain and the coiled-coil domain of SNAREs also decreases fusion efficiency, implying that the distance of complex formation from the membrane is a general critical factor for protein-mediated fusion.

Our hypothesis that stable atlastin dimerization requires the 3HB domain differs from the interpretation of the structural data on atlastin-1, which suggest that dimerization occurs through the GTPase domain (see Introduction 3.4). We have shown that, unlike atlastin fragments containing the middle domain, the isolated GTPase domain does not dimerize even in the presence of GTP *in vitro*. Further, atl(1-422), but not atl(1-328), acts as an inhibitor of membrane fusion *in vitro* and in cell culture. Presumably owing to the inability to oligomerize, atl(1-328) does not hydrolyze GTP, yet inclusion of the 3HB switches the protein to an efficient GTPase, likely because of newly acquired oligomerization ability. *In vitro* solution experiments found that both atlastin-1 and atlastin only dimerize in the presence of non- hydrolyzable GTP, yet all reported atlastin-1 dimer structures are GDP-bound (see Introduction 3.4), making it unclear which functional states these crystals represent. Alternatively, species-specific differences in protein structure may account for the observed discrepancies because atlastin-1 mediated proteoliposome fusion has yet to be demonstrated.

Our findings reveal important mechanistic insights into the functional properties of atlastin and suggest a model for atlastin-mediated homotypic fusion of ER membranes. Upon nucleotide binding, atlastin inserted within the ER membrane undergoes a conformational change that reorients the 3HB, making it available for interaction with the 3HB from a similarly primed atlastin molecule. Formation of a trans-complex induced by assembly of the 3HBs pulls the two membranes into very close apposition. The energy released after GTP hydrolysis is transduced to the lipid bilayers, resulting in their destabilization. The combination of close proximity and membrane destabilization then drives the fusion reaction. Release of the nucleotide could lead to complex disassembly, and another cycle would be prompted by binding of a new GTP molecule. Our studies support a mode of membrane fusion that uses GTP binding to drive a conformational rearrangement that promotes membrane tethering and the chemical energy of GTP hydrolysis to merge opposing phospholipid bilayers.

Finally, we report that ER membrane remodeling in *Drosophila* could be mediated also by Rtnl1 and DP1. The presence in the *Drosophila* genome of a single high conserved Reticulon and DP1 ortholog combined with the wide array of experimental tools available, makes *Drosophila* a valuable system to investigate a potential genetic and/or

functional interaction between atlastin, reticulon and Dp1. Modulation of Rtnl1 and DP1 expression *in vivo* markedly affects atlastin loss and gain of function phenotypes. Genetic elimination of $Rtnl^{1}$ in the atl^{2} null background rescues lethality and fully recuperates ER fragmentation, showing that the fragmentation observed upon loss of atlastin function is due to the activity of Rtnl1. In the fly eye, overexpression of DP1 results in a total rescue of the small eye produced by atlastin overexpression and in COS-7 cells excessive ER fusion caused by transfected atlastin is suppressed by co-expression of Rtnl1 or DP1. This strong, antagonistic interaction between atlastin, DP1, and Rtnl1 suggests that the encoded proteins exert opposing functions in the regulation of ER architecture. We propose that in the ER DP1 and Rtnl1 complements atlastin-mediated fusion. These *in vivo* data support the hypothesis that Rtnl1 and DP1 functions to counterbalance atlastin fusogenic activity perhaps by mediating membrane fission to dynamically maintain overall ER morphology.

Our studies have discovered that a three helix bundle within the middle domain and a conserved region of the C-terminal cytoplasmic tail are absolutely required for the homotypic fusion of ER membranes. We have also identified two classes of protein, reticulon and DP1, which interact with atlastin. *In vivo* and *in vitro* experiment have demonstrated that reticulon and DP1 act in a strong antagonistic manner in contrast to atlastin. Further studies will be necessary to investigate the specific mechanisms by which these proteins can drive the two oppositely directed reactions of membrane remodeling, along with advances in understanding the molecular mechanisms of action of specific fusion and fission proteins and the physics of lipid bilayer rearrangements.

5 REFERENCES

Allan VJ and Vale RD (1991) Cell cycle control of microtubule-based membrane transport and tubule formation *in vitro*. *J. Cell Biol.* **113**, 346–359

Bian X, Klemm RW, Liu TY, Zhang M, Sun S, Sui X, Liu X, Rapoport TA, Hu J (2011) Structures of the atlastin GTPase provide insight into homotypic fusion of endoplasmic reticulum membranes. *Proc Natl Acad Sci U S A.* **108**, 3976-81

Byrnes LJ, Sondermann H (2011) Structural basis for the nucleotide-dependent dimerization of the large G protein atlastin-1/SPG3A. *Proc Natl Acad Sci U S A.* **108**, 2216-21

Cauchi RJ, van den Heuvel M (2006) The fly as a model for neurodegenerative diseases: is it worth the jump? *Neurodegener Dis.* **3**, 338-56

Chan DC (2012) Fusion and fission: interlinked processes critical for mitochondrial health. *Ann Rev. Gen.* **46**, 265-87

Chan HY, Bonini NM. (2000) *Drosophila* models of human neurodegenerative disease. *Cell Death Differ.*, **7**, 1075-80

Chappie JS, Acharya S, Leonard M, Schmid SL, Dyda F (2010) G domain dimerization controls dynamin's assembly-stimulated GTPase activity. *Nature* **465**, 435-40

Collas, I. and Courvalin, J.C. (2000) Sorting nuclear membrane proteins at mitosis. *Trends Cell Biol.* **10**, 5–8

Collins RN (2006) How the ER stays in shape. *Cell* **124**, 2006

Dayel MJ and Verkman AS (1999) Diffusion of green fluorescent protein in the aqueous-phase lumen of the endoplasmic reticulum. *Biophys. J.* **76**, 2843– 2851

Ellenberg J, Siggia ED, Moreira JE, Smith CL, Presley JF, Worman HJ and Lippincott-Schwartz J. (1997) Nuclear membrane dynamics and reassembly in living cells: targeting of inner nuclear membrane protein in interphase and mitosis. *J. Cell Biol.* **138**, 1193–1206

Farhan H, Hauri HP (2009) Membrane biogenesis: networking at the er with atlastin. *Curr Biol.* **19**, 906-8

Fassier C, Hutt JA, Scholpp S, Lumsden A, Giros B, Nothias F, Schneider-Maunoury S, Houart C, Hazan J (2010) Zebrafish atlastin controls motility and spinal motor axon architecture via inhibition of the BMP pathway. *Nat Neurosci.* **13**, 1380-7

Gant TM and Wilson KL (1997) Nuclear assembly. *Annu. Rev. Cell Dev. Biol.* **13**, 695–699

Hu J, Shibata Y, Voss C, Shemesh T, Li Z, Coughlin M, Kozlov MM, Rapoport TA, Prinz WA (2008) Membrane proteins of the endoplasmic reticulum induce high-curvature tubules. *Science* **319**, 1247-50

Hu J, Shibata Y, Zhu PP, Voss C, Rismanchi N, Prinz WA, Rapoport TA, Blackstone C (2009) A class of dynamin-like GTPases involved in the generation of the tubular ER network. *Cell*. **138**, 549-61

Jackson GR (2008) Guide to understanding *Drosophila* models of neurodegenerative diseases. *PLoS Biol.* **6**, 53

Jeibmann A, Paulus W (2009) *Drosophila melanogaster* as a model organism of brain diseases. *Int J Mol Sci.* **10**, 407-40

Koch GLE and Booth C (1988) Dissociation and re-assembly of the endoplasmic reticulum in live cells. *J. Cell Sci.* **91**, 511–522

Kozlov MM, McMahon HT, Chernomordik LV (2010) Protein-driven membrane stresses in fusion and fission. *Trends Biochem Sci.* **35,** 699-706

Lazar NL, Singh S, Paton T, Clapcote SJ, Gondo Y, Fukumura R, Roder JC, Cain DP (2011) Missense mutation of the reticulon-4 receptor alters spatial memory and social interaction in mice. *Behav Brain Res.* **10,** 73-9

Lee M, Paik SK, Lee M-J, Kim Y-K, Kim S, Nahm M, Oh S-J, Kim H-M, Yim J, Justin Lee C, Bae YC, Lee S (2009) *Drosophila* Atlastin regulates the stability of muscle microtubules and is required for synapse development. *Developmental Biology* **330**, 250–262

Liu T, Bian X, Sun S, Hu X, Klemm RX, Prinz WA, Rapoport TA and Hu J (2012) Lipid interaction of the C terminus and association of the transmembrane segments facilitate atlastin-mediated homotypic endoplasmic reticulum fusion. *PNAS* **109**, 2146-54

Martens S, McMahon HT (2008) Mechanisms of membrane fusion: disparate players and common principles. *Nat Rev Mol Cell Biol.* **9,** 543-56

McMahon HT, Gallop JL (2005) Membrane curvature and dynamic cell membrane remodelling. *Nature* **1,** 590-6.

McNew JA, Weber T, Engelman DM, Söllner TH, Rothman JE. (1999) The length of the flexible SNAREpin juxtamembrane region is a critical determinant of snare-dependent fusion. *Mol Cell.* **4**, 415-21

Montenegro G, Rebelo AP, Connell J, Allison R, Babalini C, D'Aloia M, Montieri P, Schüle R, Ishiura H, Price J, Strickland A, Gonzalez MA, Baumbach-Reardon L, Deconinck T, Huang J, Bernardi G, Vance JM, Rogers MT, Tsuji S, De Jonghe P, Pericak-Vance MA, Schöls L, Orlacchio A, Reid E, Züchner S. (2012) Mutations in the ER-shaping protein reticulon 2 cause the axon-degenerative disorder hereditary spastic paraplegia type 12. *J Clin Invest.* **122**, 538-44

Morin-Leisk J, Saini SG, Meng X, Makhov AM, Zhang P, Lee TH (2011) An intramolecular salt bridge drives the soluble domain of GTP-bound atlastin into the postfusion conformation. *J Cell Biol.* **195**, 605-15

Moss TJ, Andreazza C, Verma A, Daga A, McNew JA (2011) Membrane fusion by the GTPase atlastin requires a conserved C-terminal cytoplasmic tail and dimerization through the middle domain. *Proc Natl Acad Sci U S A.* **108**, 11133-8

Moss TJ, Daga A, McNew JA (2011) Fusing a lasting relationship between ER tubules. *Trends Cell Biol.* **21**, 416-23

Muriel MP, Dauphin A, Namekawa M, Gervais A, Brice A, Ruberg M (2009) Atlastin-1, the dynamin-like GTPase responsible for spastic paraplegia SPG3A, remodels lipid membranes and may form tubules and vescicles in the endoplasmic reticulum . *J Neurochem.* **110**, 1607-16

Namekawa M, Muriel MP, Janer A, Latouche M, Dauphin A, Debeir T, Martin E, Duyckaerts C, Prigent A, Depienne C, Sittler A, Brice A, Ruberg M (2007) Mutations in the SPG3A gene encoding the GTPase atlastin interfere with vesicle trafficking in the ER/Golgi interface and Golgi morphogenesis. Mol Cell Neurosci. **35,** 1-13

Orso G, Pendin D, Liu S, Tosetto J, Moss TJ, Faust JE, Micaroni M, Egorova A, Martinuzzi A, McNew JA, Daga A (2009) Homotypic fusion of ER membranes requires the dynamin-like GTPase Atlastin. *Nature* **460**, 978-83

O'Sullivan NC, Jahn TR, Reid E and O'Kane CJ (2012) Reticulon-like-1, the *Drosophila* orthologue of the Hereditary Spastic Paraplegia gene reticulon 2, is required for organization of endoplasmic reticulum and of distal motor axons. *Hum. Mol. Gen.* **21**, 3356-65

Park SH & Blackstone C (2010) Further assembly required: construction and dynamics of the endoplasmic reticulum network. *EMBO Rep*.**11**, 515-21

Park SH, Zhu PP, Parker RL, Blackstone C (2010) Hereditary spastic paraplegia proteins REEP1, spastin, and atlastin-1 coordinate microtubule interactions with the tubular ER network. *J Clin Invest*. **120**, 1097-110

Pendin D, McNew JA, Daga A (2011) ER dynamics: shaping, bending, severing, and mending membranes. *Curr Opin Cell Biol.* **23**, 435-42

Pendin D, Tosetto J, Moss TJ, Andreazza C, Moro S, McNew JA, Daga A (2011) GTP-dependent packing of a three-helix bundle is required for atlastin-mediated fusion. *Proc Natl Acad Sci U S A*. **108**, 16283-8

Prinz, W.A., Grzyb, L., Veenhuis, M., Kahana, J.A., Silver, P.A. and Rapoport, T.A (2000) Mutants affecting the structure of the cortical endoplasmic reticulum in *Saccharomyces cerevisiae*. *J. Cell Biol.* **150**, 461–474

Rismanchi N, Soderblom C, Stadler J, Zhu PP, Blackstone C (2008) Atlastin GTPases are required for Golgi apparatus and ER morphogenesis. *Hum Mol Genet.* **17**, 1591-604

Rong YS and Golic KG (2001) A targeted gene knockout in *Drosophila. Genetics* **157**, 1307-1312

Rossetto MG, Zanarella E, Orso G, Scorzeto M, Megighian A, Kumar V, Delgado-Escueta AV and Daga A (2011) Defhc1.1, a homologue of the juvenile myoclonic gene EFHC1, modulates architecture and basal activity of the neuromuscular junction in *Drosophila*. *Hum. Mol. Gen*. **21,** 4249

Roux A, Koster G, Lenza M, Sorre B, Manneville J-B, Nassoy P, and Bassereau P (2010) Membrane curvature controls dynamin polymerization. *PNAS* **107**, 4141-4146

Shibata Y, Voss C, Rist JM, Hu J, Rapoport TA, Prinz WA, Voeltz GK (2008) The reticulon and DP1/YOP1p proteins form immobile oligomers in the tubular endoplasmic reticulum. *J Biol Chem.* **283**, 18892-904

Teng FYU and Tang BL (2008) Cell autonomous function of Nogo and Reticulons: the emerging story at the endoplasmic reticulum. *J. Cell. Physiol.* **216**, 303-308

Terasaki, M (2000) Dynamics of the endoplasmic reticulum and Golgi apparatus during early sea urchin development. *J. Cell Biol.* **114**, 929–940

Terasaki M, Chen LB and Fujiwara K (1986) Microtubules and the endoplasmic reticulum are highly interdependent structures. *J. Cell Biol.* **103**, 1557–1568

Terasaki M and Jaffe LA (1991) Organization of the sea urchin egg endoplasmic reticulum and its reorganization at fertilization. *J. Cell Biol.* **114**, 929–940

Terasaki M, Slater NT, Fein A, Schmidek A and Reese TS (1994) Continuous network of endoplasmic reticulum in cerebellar Purkinje neurons. *Proc. Natl Acad. Sci. USA*, **91**, 7510–7514

Tolley N, Sparkes I, Craddock CP, Eastmond PJ, Runions J, Hawes C, Frigerio L (2010) Transmembrane domain length is responsible for the ability of a plant reticulon to shape endoplasmic reticulum tubules *in vivo*. *Plant J.* **64**, 411-8

Tolley N, Sparkes IA, Hunter PR, Craddock CP, Nuttall J, Roberts LM, Hawes C, Pedrazzini E, Frigerio L (2008) Overexpression of a plant reticulon remodels the lumen of the cortical endoplasmic reticulum but does not perturb protein transport. *Traffic* **9**, 94-102

Voeltz GK, Prinz WA, Shibata Y, Rist JM, Rapoport TA (2006) A class of membrane proteins shaping the tubular endoplasmic reticulum . *Cell* **124**, 573-86

Voeltz GK, Rolls MM, Rapoport TA (2002) Structural organization of the endoplasmic reticulum. *EMBO Rep.* **3**, 944-50

Wakefield S, Tear G (2006) The *Drosophila* reticulon, Rtnl-1, has multiple differentially expressed isoforms that are associated with a sub-compartment of the endoplasmic reticulum. *Cell Mol Life Sci.* **63**, 2027-38

Waterman-Storer CM and Salmon ED (1998) Endoplasmic reticulum membrane tubules are distributed by microtubules in living cells using three distinct mechanisms. *Curr. Biol.* **8**, 798–806

Weber T, Zemelman BV, McNew JA, Westermann B, Gmachl M, Parlati F, Söllner TH, Rothman JE (1998) SNAREpins: Minimal Machinery for Membrane Fusion. *Cell*. **92**, 759-72

Yang YS, Strittmatter SM (2007) The reticulons: a family of proteins with diverse functions. *Genome Biol.* **8**, 234

Zimmerberg J, Kozlov MM (2006) How proteins produce cellular membrane curvature. *Nat Rev Mol Cell Biol.* **7**, 9-19

Zhu PP, Patterson A, Lavoie B, Stadler J, Shoeb M, Patel R, Blackstone C (2003) Cellular localization, oligomerization, and membrane association of the hereditary spastic paraplegia 3a (SPG3A) protein atlastin. *J Biol Chem.* **278**, 49063-71

Zhu PP, Soderblom C, Tao-Cheng JH, Stadler J, Blackstone C (2006) SPG3A protein atlastin-1 is enriched in growth cones and promotes axon elongation during neuronal development. *Hum Mol Genet.* **15,** 1343-53

Zurek N, Sparks L, Voeltz G (2011) Reticulon Short Hairpin Transmembrane Domains Are Used to Shape ER Tubules. *Traffic* **12**, 28-41

Acknowledgements

Thanks to Andrea Daga and all the people of the laboratory.

Thanks to James A. McNew's laboratory for *in vitro* experiments.

Thanks to Stefano Moro for molecular modeling.

Thanks to Vadim A. Frolov's laboratory for liposome experiments and analysis of the endoplasmic reticulum network.